



PROCUREMENT EXECUTIVE, MINISTRY OF DEFENCE

AERONAUTICAL RESEARCH COUNCIL

REPORTS AND MEMORANDA

Linearized Supersonic Unsteady Flow in Cascades

By T. NAGASHIMA AND D. S. WHITEHEAD

University Engineering Department, Cambridge

1978
AERONAUTICAL RESEARCH COUNCIL
REPORTS AND MEMORANDA

LONDON: HER MAJESTY'S STATIONERY OFFICE

1978

£4 net

Linearized Supersonic Unsteady Flow in Cascades

By T. NAGASHIMA AND D. S. WHITEHEAD

University Engineering Department, Cambridge

*Reports and Memoranda No. 3811**

February, 1977

Summary

A linearised theory is presented for the calculation of force and moment coefficients for two-dimensional cascades of blades in supersonic flow. The cases of both supersonic and subsonic axial velocity are treated. The perturbations are due to bending vibration, torsional vibration, and wakes shed from moving obstructions upstream. The method leads to analytical results in the quasi-steady case, and to a fast computer program for the general unsteady case. Results are in good agreement with previous work. The method can be used to predict forced vibration and flutter in transonic fan blades.

* Replaces A.R.C. 37 198

LIST OF CONTENTS

1. Introduction
2. Basis of The Theory
3. Calculation of the Kernel Function
4. Effect of Wave Reflections
5. Numerical Solutions of Integral Equations
6. Steady Solutions
7. Quasi-Steady Solutions
8. Results and Comparison with Other Work
9. Conclusions

List of Symbols

References

Tables 1 to 2

Illustrations: Figs. 1 to 13

Detachable Abstract Cards

1. Introduction

In the development of high performance compressors and turbines for aviation applications, the problem of blade vibration has been one of the most persistent and troublesome. This is because the need to minimise the weight of the machine leads to slender blading which is prone to vibration. In particular, the fan blading on modern fan engines has encountered severe flutter in a mode in which the blade motion includes both bending and torsion, and the blades are coupled together through their snubbers. This type of flutter has been described by Snyder and Commerford (1974)¹⁶ and by Halliwell (1976)⁵. The flutter occurs when the blade tips have a supersonic relative inlet Mach number and are not stalled. There is a pressing need to be able to predict this type of flutter, and there is also great interest in predicting the amplitude of vibration that will be forced by wakes or other kinds of maldistribution in the inlet flow.

In the construction of a prediction method, it is necessary to use a number of simplifying assumptions in the development of the theory. All available supersonic theories are two-dimensional, and this assumption will be made here. Namba (1976)¹¹ has shown that in a three-dimensional subsonic situation the two-dimensional unsteady strip theory works well, so that there is good reason to hope that strip theory can be extended to apply to fans with supersonic tips.

It will also be assumed that the unsteady effects are small perturbations of a uniform flow with a supersonic Mach number. Thus all effects due to incidence, lift, camber, thickness, and shock waves are neglected. It appears that flutter of actual fan blades running at a given speed is worst when the pressure rise through the fan is least. The neglect of the effect of the pressure rise is therefore likely to lead to a conservative estimate of the flutter susceptibility of the fan. It will also be assumed that all blades vibrate with the same amplitude and with a constant phase angle ϕ between each blade and its neighbour. Both flutter and forced vibration of identical blades is of this form, but in fact any motion of a blade row can be synthesised by superposing components of this kind, so that the assumption does not lead to any loss of generality. The object of this report is therefore to predict the aerodynamic forces and moments acting on a cascade of vibrating flat plates, due to (a) translational vibration of the plates normal to their chord lines, corresponding to bending vibration of a three-dimensional blade, (b) torsional motion about a given axis, and (c) wakes convected into the cascade from some other obstruction upstream. This is the basic aerodynamic data necessary to predict both flutter and forced vibration.

The nature of the solution is fundamentally different according to whether the axial velocity is subsonic or supersonic. In all practical turbomachines the axial velocity is subsonic, and therefore this case is of primary interest. In this case it is possible for information to be transmitted upstream in an axial direction, and the situation therefore combines some features of subsonic flow with some features of supersonic flow. But the case when the axial velocity is supersonic is much easier to treat theoretically, and this was the first case to be studied.

The problem of wall interference for a single aerofoil oscillating in a wind tunnel, which corresponds to an unstaggered cascade with antiphase oscillation of the blades, has been investigated by Drake (1957)². The unstaggered cascade with arbitrary phase angle was analysed by Lane (1957)⁹ using Laplace transform techniques. The case of supersonic axial velocity has also been analysed by Gorelov (1966)⁴ and by Platzer and Chalkley (1972)¹⁴ who used the method of characteristics. Nishiyama and Kikuchi (1973)¹² have reported a theory based on the image method.

Turning to the case of subsonic axial velocity, this was considered by Gorelov (1966)⁴ but no numerical results were obtained. An analysis for a finite cascade was given by Verdon (1973)¹⁷, in which blades were added to a finite cascade until no further significant change in the flow pattern was obtained. Kurosaka (1973)⁸ gave a quasi-steady solution, valid for low frequency parameters. Brix and Platzer (1974)¹ have used the method of characteristics, and obtained reasonably good agreement with Verdon (1973)¹⁷ for a finite cascade. An analysis by Verdon and McCune (1975)¹⁸ for an infinite cascade gives the most comprehensive results available to date. A comparison between the finite cascade and infinite cascade assumptions has been made by Platzer, Chadwick, and Schlein (1976)¹³, who also developed an infinite cascade theory which showed good agreement with the results of Verdon and McCune (1975)¹⁸. Platzer, Chadwick, and Schlein (1976)¹³ find that as the number of blades used in the finite cascade analysis increases, the results for lift and moment converge towards the results of the infinite cascade analysis, but the results for the individual surface pressures do not converge.

In most of the above analyses, including that by Verdon and McCune (1975)¹⁸, the solution is obtained in terms of the velocity potential. Here, it is preferred to work in terms of the pressure (or acceleration potential), since there are then no source terms arising from the wakes of the blades, due to the vorticity shed from the trailing edges.

The method of solution used in the present report is very similar to that proposed independently by Goldstein (1975)³. However, Goldstein's paper does not take the solution so far as to obtain any results.

2. Basis of The Theory

In setting up the basic equations of motion, it is convenient to regard the force applied to the fluid by the blades as a generalised body force (\mathbf{F}) per unit mass, which could be distributed over the whole field.

The thin-aerofoil assumption is made, that the deviations from a uniform flow with velocity U are small, so that the equations may be linearised and are as follows:—

Continuity

$$\frac{D\rho}{Dt} + \rho_0 \nabla \cdot v = 0. \quad (1)$$

Momentum

$$\frac{Dv}{Dt} + \frac{1}{\rho_0} \nabla p = \mathbf{F}. \quad (2)$$

Isentropic flow

$$\frac{p}{\rho} = \frac{\gamma p_0}{\rho_0} = a_0^2. \quad (3)$$

The solution will be constructed in terms of the pressure, p . From equations (1), (2) and (3), this satisfies the convected wave equation with a source term on the right hand side,

$$\left(\nabla^2 - \frac{1}{a_0^2} \frac{D^2}{Dt^2} \right) p = \rho_0 \nabla \cdot \mathbf{F}. \quad (4)$$

The case of interest is when all variables oscillate with angular frequency ω . Hence the body force is of the form:

$$\mathbf{F}(t, x, y) = \mathbf{F}(x, y) e^{i\omega t},$$

and similarly,

$$p(t, x, y) = p(x, y) e^{i\omega t}.$$

Then equation (4) becomes

$$\left\{ -(M^2 - 1) \frac{\partial^2}{\partial x^2} + \frac{\partial^2}{\partial y^2} - \frac{2i\omega U}{a_0^2} \frac{\partial}{\partial x} + \frac{\omega^2}{a_0^2} \right\} p(x, y) = \rho_0 \nabla \cdot \mathbf{F}(x, y). \quad (5)$$

This body force is applied by the thin blades, in the y direction normal to the blade surface. Thus each blade is considered as being replaced by pressure dipoles distributed along the chord. The origin of co-ordinates is taken at the mid point of the reference blade ($m=0$), and extends from $x = -c/2$ to $x = +c/2$. Hence the body force corresponding to the reference blade has only a y component which is

$$\mathbf{F}_0(x, y) = -\frac{1}{\rho_0} f(x) \delta(y),$$

where $f(x)$ is the distribution of lift force along the chord of the reference blade, and the minus sign is because the lift force on the blade is taken positive in the y direction.

The m th blade has its mid-chord point at $x = ms \sin \theta$, $y = ms \cos \theta$. Also, it is assumed that there is a constant phase angle ϕ between each blade and the one below it. Hence the body force due to the m th blade is

$$\begin{aligned} \mathbf{F}_m(x, y) &= \mathbf{F}_0(x - ms \sin \theta, y - ms \cos \theta) e^{im\phi} \\ &= -(1/\rho_0) f(x - ms \sin \theta) \delta(y - ms \cos \theta) e^{im\phi}. \end{aligned}$$

Summing for all blades, the force field is

$$\mathbf{F}(x, y) = -(1/\rho_0) \sum_{m=-\infty}^{+\infty} f(x - ms \sin \theta) \delta(y - ms \cos \theta) e^{im\phi}. \quad (6)$$

The solution of equation (5) may be expressed as

$$p(x, y) = \iint \rho_0 \nabla \mathbf{F}(\xi, \eta) G(x - \xi, y - \eta) d\xi d\eta, \quad (7)$$

where G is the Green's function of equation (5).

Substituting equations (6) into (7), and evaluating the integral over η by parts gives

$$p(x, y) = - \int_{-c/2}^{+c/2} f(\xi) d\xi \sum_{m=-\infty}^{+\infty} e^{im\theta} \frac{\partial}{\partial y} \{G(x - \xi - ms \sin \theta, y - ms \cos \theta)\}. \quad (8)$$

Once the pressure has been found, the velocity perturbations can be found from equation (2). For harmonic oscillation and in any region where the body force is zero, this gives

$$\left(i\omega + U \frac{\partial}{\partial x}\right) u = - \frac{1}{\rho_0} \frac{\partial p}{\partial x}, \quad (9)$$

$$\left(i\omega + U \frac{\partial}{\partial x}\right) v = - \frac{1}{\rho_0} \frac{\partial p}{\partial y}. \quad (10)$$

The distribution of pressure dipoles along the chord, $f(\xi)$, has to be arranged so that the induced velocity normal to the surface of the blades, v_i , given by equation (10), matches the required upwash velocity v_U , so that

$$v_i = v_U. \quad (11)$$

Three kinds of upwash will be considered. These are (a) Bending vibration of the blades with velocity $q \exp(i\omega t)$, so that

$$v_U = q. \quad (12)$$

(b) Torsional motion of the blades with angular displacement $\alpha \exp(i\omega t)$, positive nose down, about an axis position given by x_η . Matching the vibration normal to the surface gives

$$(v_i - U\alpha) e^{i\omega t} = (x - x_\eta) \frac{\partial}{\partial t} (\alpha e^{i\omega t}),$$

so that

$$v_U = U\alpha \{1 + i\omega(x - x_\eta)/U\}. \quad (13)$$

(c) The effect of wakes from any kind of periodic obstruction upstream is calculated. These wakes involve a vorticity perturbation, but no pressure perturbation, so that they are convected downstream at the main-stream velocity U . The amplitude of the wakes will be specified by the velocity which the wakes would induce at the position of the mid-chord point of the reference blade, if the cascade were removed, which is $-w \exp(i\omega t)$. Matching the velocities normal to the surface gives

$$v_i e^{i\omega t} - w e^{i\omega(t-x/U)} = 0,$$

so that

$$v_i = w e^{-i\omega x/U} \quad (14)$$

This known upwash velocity enables an integral equation to be set up to calculate the unknown distribution of pressure dipoles along the chord, given by f . The calculation of the kernel function of the integral equation is considered in the next section.

Once f is known, the lift on the aerofoil is given by

$$L = \int_{-c/2}^{+c/2} f(\xi) d\xi. \quad (15)$$

The moment about the torsional axis at $x = x_\eta$, taken nose down positive, is

$$M_\alpha = \int_{-c/2}^{+c/2} f(\xi)(\xi - x_\eta) d\xi. \quad (16)$$

3. Calculation of the Kernel Function

The Green's function of equation (5) can be obtained by solving the equation

$$\left\{ -(M^2 - 1) \frac{\partial^2}{\partial x^2} + \frac{\partial^2}{\partial y^2} - \frac{2i\omega U}{a_0^2} \frac{\partial}{\partial x} + \frac{\omega^2}{a_0^2} \right\} G(x, y) = \delta(x)\delta(y). \quad (17)$$

This equation has to be solved subject to the boundary condition that there is no disturbance outside the Mach cone emanating from the origin.

This boundary condition will be handled by the mathematical device of supposing that the angular frequency ω has a small negative imaginary part, so that

$$\omega = \omega_1 - i\omega_2$$

where ω_1 and ω_2 are real and positive, and the limit $\omega_2 \rightarrow 0$ is implied. This means physically that an oscillation which is growing very slowly in time is being studied. Disturbances which originate far from the reference blade must have been emitted at much earlier times when the oscillation was negligible small. Hence this device eliminates unwanted effects coming from the far field.

The solution is sought in the form of a double Fourier transform as follows

$$G(x, y) = \frac{1}{4\pi^2} \int_{-\infty}^{+\infty} e^{-i\lambda x} d\lambda \int_{-\infty}^{+\infty} \tilde{G}(\lambda, \alpha) e^{-i\alpha y} d\alpha. \quad (18)$$

The Dirac delta functions in equation (17) can be similarly expressed as

$$\delta(x) = \frac{1}{2\pi} \int_{-\infty}^{+\infty} e^{-i\lambda x} d\lambda, \quad (19)$$

$$\delta(y) = \frac{1}{2\pi} \int_{-\infty}^{+\infty} e^{-i\alpha y} d\alpha. \quad (20)$$

Substituting equations (18), (19) and (20) in equation (17) gives

$$\left\{ (M^2 - 1)\lambda^2 - \alpha^2 - \frac{2\omega U}{a_0^2} \lambda + \frac{\omega^2}{a_0^2} \right\} \tilde{G}(\lambda, \alpha) = 1.$$

This may be written

$$\{B^2(\lambda - \bar{\mu}/c)^2 - \alpha^2 - B^2\bar{\kappa}^2/c^2\} \tilde{G}(\lambda, \alpha) = 1,$$

where $B^2 = M^2 - 1$,

$$\bar{\omega} = \omega c / U,$$

$$\bar{\kappa} = M\bar{\omega} / B^2,$$

$$\bar{\mu} = M\bar{\kappa}.$$

Hence the Green's function is given by

$$G(x, y) = \frac{1}{4\pi^2} \int_{-\infty}^{+\infty} e^{-i\lambda x} d\lambda \int_{-\infty}^{+\infty} \frac{e^{-i\alpha y} d\alpha}{B^2(\lambda - \bar{\mu}/c)^2 - \alpha^2 - B^2\bar{\kappa}^2/c^2}$$

It will be convenient to replace λ by a displaced variable $\lambda' = \lambda - \bar{\mu}/c$, so that

$$G(x, y) = \frac{1}{4\pi^2} e^{-i\bar{\mu}x/c} \int_{-\infty - \bar{\mu}/c}^{+\infty - \bar{\mu}/c} e^{-i\lambda'x} d\lambda' \int_{-\infty}^{+\infty} \frac{e^{-i\alpha y} d\alpha}{B^2\lambda'^2 - \alpha^2 - B^2\bar{\kappa}^2/c^2}. \quad (21)$$

If ω and therefore $\bar{\mu}$ are real, the displacement by $\bar{\mu}/c$ on the limits of the first integral makes no difference. But since ω is supposed to have a small negative imaginary part, it will be necessary to allow for this in the evaluation of this integral.

At this point it is convenient to switch to a non-dimensional co-ordinate system, and to work in a transformed plane (\bar{x}, \bar{y}) . The relationships are as follows

$$\begin{aligned}\bar{x} &= x/c, \quad \bar{\xi} = \xi/c, \quad \bar{\lambda} = c\lambda', \\ \bar{y} &= By/c, \quad \bar{\eta} = B\eta/c, \quad \bar{\alpha} = \alpha/B, \\ \tan \bar{\theta} &= (\tan \theta)/B, \\ \bar{s} &= (sB \cos \theta)/(c \cos \theta).\end{aligned}\tag{22}$$

In this plane the Mach waves propagate at 45° to the \bar{x}, \bar{y} axes.

Equation (21) becomes

$$\bar{G}(\bar{x}, \bar{y}) = BG(x, y) = \frac{1}{4\pi^2} e^{-i\bar{\mu}\bar{x}} \int_{-\infty-\bar{\mu}}^{+\infty-\bar{\mu}} e^{-i\bar{\lambda}\bar{x}} d\bar{\lambda} \int_{-\infty}^{+\infty} \frac{e^{-i\bar{\alpha}\bar{y}} d\bar{\alpha}}{\bar{\lambda}^2 - \bar{\alpha}^2 - \bar{\kappa}^2}.\tag{23}$$

Equation (8) becomes

$$\bar{p}(\bar{x}, \bar{y}) = \int_{-1/2}^{+1/2} \bar{f}(\bar{\xi}) \bar{p}_\xi(\bar{x} - \bar{\xi}, \bar{y}) d\bar{\xi},\tag{24}$$

where

$$\bar{p}_\xi(\bar{x}, \bar{y}) = \sum_{m=-\infty}^{+\infty} e^{-i\bar{\mu}\bar{x}_m + im\phi} \frac{1}{4\pi^2} \int_{-\infty-\bar{\mu}}^{+\infty-\bar{\mu}} e^{-i\bar{\lambda}\bar{x}_m} d\bar{\lambda} \int_{-\infty}^{+\infty} \frac{i\bar{\alpha} e^{-i\bar{\alpha}\bar{y}_m} d\bar{\alpha}}{\bar{\lambda}^2 - \bar{\alpha}^2 - \bar{\kappa}^2},\tag{25}$$

and

$$\begin{aligned}\bar{p} &= p/\rho_0 U^2, \quad \bar{f} = f/\rho_0 U^2, \\ \bar{x}_m &= \bar{x} - m\bar{s} \sin \bar{\theta}, \quad \bar{y}_m = \bar{y} - m\bar{s} \cos \bar{\theta}.\end{aligned}$$

This shows how the solution for the pressure is constructed from the strength of the dipole sources distributed along the reference blade.

The corresponding expressions for the velocity perturbations may be obtained from equations (9) and (10) and are

$$\bar{u}(\bar{x}, \bar{y}) = \frac{u(x, y)}{U} = \int_{-1/2}^{+1/2} \bar{f}(\bar{\xi}) \bar{u}_\xi(\bar{x} - \bar{\xi}, \bar{y}) d\bar{\xi},\tag{26}$$

$$\bar{v}(\bar{x}, \bar{y}) = \frac{v(x, y)}{BU} = \int_{-1/2}^{+1/2} \bar{f}(\bar{\xi}) \bar{v}_\xi(\bar{x} - \bar{\xi}, \bar{y}) d\bar{\xi},\tag{27}$$

where

$$\bar{u}_\xi(\bar{x}, \bar{y}) = - \sum_{m=-\infty}^{+\infty} e^{-i\bar{\mu}\bar{x}_m + im\phi} \frac{1}{4\pi^2} \int_{-\infty-\bar{\mu}}^{+\infty-\bar{\mu}} \frac{(\bar{\lambda} + \bar{\mu}) e^{-i\bar{\lambda}\bar{x}_m} d\bar{\lambda}}{(\bar{\lambda} + \bar{\omega}/B^2)} \int_{-\infty}^{+\infty} \frac{i\bar{\alpha} e^{-i\bar{\alpha}\bar{y}_m} d\bar{\alpha}}{(\bar{\lambda}^2 - \bar{\alpha}^2 - \bar{\kappa}^2)},\tag{28}$$

$$\bar{v}_\xi(\bar{x}, \bar{y}) = - \sum_{m=-\infty}^{+\infty} e^{-i\bar{\mu}\bar{x}_m + im\phi} \frac{1}{4\pi^2} \int_{-\infty-\bar{\mu}}^{+\infty-\bar{\mu}} \frac{e^{-i\bar{\lambda}\bar{x}_m} d\bar{\lambda}}{(\bar{\lambda} + \bar{\omega}/B^2)} \int_{-\infty}^{+\infty} \frac{i\bar{\alpha}^2 e^{-i\bar{\alpha}\bar{y}_m} d\bar{\alpha}}{(\bar{\lambda}^2 - \bar{\alpha}^2 - \bar{\kappa}^2)}.\tag{29}$$

Equations (28) and (29) show that in the $\bar{\lambda}$ integration an additional pole appears at $\bar{\lambda} = -\bar{\omega}/B^2$. This corresponds physically to vorticity waves which are convected downstream at a speed U , and which do not involve any pressure perturbation.

The integrals in equations (25), (28) and (29) can be evaluated in terms of the Bessel function J_0 to give the form

$$\bar{p}_\xi(\bar{x}, \bar{y}) = - \sum_{m=-\infty}^{+\infty} e^{-i\bar{\mu}\bar{x}_m + im\phi} \frac{\partial}{\partial \bar{y}} \{J_0[\bar{\kappa}(\bar{x}_m^2 - \bar{y}_m^2)^{1/2}] H(\bar{x}_m - |\bar{y}_m|)\},\tag{30}$$

where H is the Heaviside step function. However, this series shows poor convergence, and becomes unsuitable for numerical work anywhere near the acoustic resonance which will be discussed later.

If, alternatively, the series in these equations are subject to a transformation similar to the Poisson summation formula, the result is another series, which in physical terms consists of propagating or decaying acoustic waves. This technique works very well in subsonic flow (Kaji and Okazaki (1970)⁶, Smith (1972)¹⁵)

but in this case of supersonic flow the convergence is bad since all the higher order terms consist of propagating waves, and these do not decrease in amplitude.

The procedure that will be followed is therefore to split the inner factor in these equations into three terms as follows

$$\frac{1}{\lambda^2 - \bar{\alpha}^2 - \bar{\kappa}^2} = \frac{1}{\lambda^2 - \bar{\alpha}^2} + \bar{\kappa}^2 \frac{1}{(\lambda^2 - \bar{\alpha}^2)^2} + \bar{\kappa}^4 \frac{1}{(\lambda^2 - \bar{\alpha}^2)^2 (\lambda^2 - \bar{\alpha}^2 - \bar{\kappa}^2)}. \quad (31)$$

The first two terms are the first two terms of an expansion in $\bar{\kappa}^2$, or frequency parameter. These terms therefore give the low frequency behaviour, and are conveniently handled by summing over blade numbers. The last term is the remainder, and it will be transformed into a summation over propagating and decaying acoustic waves.

Since only the v velocity is required in order to set up the Kernel function, only this variable will be treated. Equation (29) is therefore written

$$\bar{v}_\xi = {}_0\bar{v}_\xi + {}_1\bar{v}_\xi + {}_2\bar{v}_\xi, \quad (32)$$

where the three terms correspond to the terms in equation (31).

The ${}_0\bar{v}_\xi$ term is obtained from equation (29), putting $\bar{\kappa} = 0$. The integrals may be evaluated by standard contour integration methods to give

$${}_0\bar{v}_\xi(\bar{x}, \bar{y}) = -\frac{1}{2} \sum_{m=-\infty}^{+\infty} e^{-i\bar{\omega}(\bar{x}_m + |\bar{y}_m|/B^2) + im\phi} \left\{ \delta(\bar{x}_m - |\bar{y}_m|) + \frac{i\bar{\omega}}{B^2} H(\bar{x}_m - |\bar{y}_m|) \right\}. \quad (33)$$

The δ function shows the disturbances propagating along the Mach lines, at 45° to the transformed axes. There is also some unsteady effect downstream of these Mach waves, given by the H function.

Similarly the ${}_1\bar{v}_\xi$ term may also be evaluated as follows

$$\begin{aligned} {}_1\bar{v}_\xi(\bar{x}, \bar{y}) &= - \sum_{m=-\infty}^{+\infty} e^{-i\bar{\mu}\bar{x}_m + im\phi} \frac{1}{4\pi^2} \int_{-\infty - \bar{\mu}}^{+\infty - \bar{\mu}} \frac{e^{-i\bar{\lambda}\bar{x}_m} d\bar{\lambda}}{(\bar{\lambda} + \bar{\omega}/B^2)} \int_{-\infty}^{+\infty} \frac{i\bar{\alpha}^2 \bar{\kappa}^2 e^{-i\bar{\alpha}\bar{y}_m} d\alpha}{(\lambda^2 - \bar{\alpha}^2)^2} \\ &= \frac{\bar{\kappa}^2}{4} \sum_{m=-\infty}^{+\infty} e^{-i\bar{\omega}(\bar{x}_m + |\bar{y}_m|/B^2) + im\phi} \left\{ |\bar{y}_m| + \frac{B^2}{i\bar{\omega}} [e^{-i\bar{\omega}(\bar{x}_m + |\bar{y}_m|/B^2)} - 1] \right\} H(\bar{x}_m - |\bar{y}_m|). \end{aligned} \quad (34)$$

These velocities need to be evaluated on the surface of the reference blade, where $-0.5 < \bar{x} < 0.5$, and $\bar{y} = 0$. The delta function in equation (33) always yields a finite number of terms in the summation over m . The other terms in equations (33) and (34) are governed by the H function, which yields the condition

$$\begin{aligned} \bar{x}_m - |\bar{y}_m| &> 0 \\ \bar{x} - m\bar{s} \sin \bar{\theta} - |m|\bar{s} \cos \bar{\theta} &> 0, \end{aligned}$$

i.e.

$$\bar{x} > m d_1 \quad \text{for } m > 0, \quad (35)$$

and

$$\bar{x} > m d_2 \quad \text{for } m \leq 0, \quad (36)$$

where

$$d_1 = \bar{s}(\sin \bar{\theta} + \cos \bar{\theta}),$$

and

$$d_2 = \bar{s}(\sin \bar{\theta} - \cos \bar{\theta}).$$

These results are illustrated physically in Fig. 2, which shows the Mach lines radiating at 45° to the transformed axes from a row of sources. If the axial velocity is supersonic, all the waves go downstream of the row, and there is no upstream effect. In this case $\bar{\theta} < 45^\circ$, d_2 is negative, and there is no effect if \bar{x} is negative. For \bar{x} positive the summation includes a finite number of terms given by

$$m^- = [\bar{x}/d_2] \leq m \leq m^+ = [\bar{x}/d_1],$$

where the square brackets indicate that the quantity enclosed is to be truncated to the nearest integer towards zero.

For the subsonic axial velocity case, Fig. 2 shows how some of the waves go upstream of the row. In this case $\bar{\theta} > 45^\circ$, d_2 is positive, and equation (35) gives

$$0 \leq m \leq m^+ \quad \text{for } \bar{x} > 0$$

and equation (36) gives

$$-\infty < m < m^- \quad \text{for } \bar{x} < 0$$

and

$$-\infty < m < 0 \quad \text{for } \bar{x} > 0.$$

In this case therefore the summation has an infinite number of terms.

These infinite summations may be evaluated by the formulae

$$\sum_{m=1}^{\infty} e^{imz} = \frac{e^{iz}}{i - e^{iz}},$$

$$\sum_{m=1}^{\infty} m e^{imz} = \frac{e^{iz}}{(1 - e^{iz})^2}, \quad \text{for } \mathcal{I}(z) > 0.$$

The condition on the imaginary part of z is satisfied, from the assumption that ω has a small negative imaginary part.

Applying these formulae to equations (32) and (34) gives, for subsonic axial velocity,

$${}_0\bar{v}_\xi(\bar{x}, 0) = -\frac{1}{2} \left\{ \sum_{m=0}^{\infty} e^{im(-\bar{\mu}\bar{s} \cos \bar{\theta} + \phi)} \delta(\bar{x} - md_1) + \sum_{m=1}^{\infty} e^{im(-\bar{\mu}\bar{s} \cos \bar{\theta} - \phi)} \delta(\bar{x} + md_2) \right\}$$

$$- \frac{i\bar{\omega}}{2B^2} e^{-i\bar{\omega}\bar{x}} \left\{ \sum_{m=1}^{m^+} e^{imC_2} - H(-\bar{x}) \sum_{m=0}^{-m^-} e^{imC_1} + \frac{1}{1 - e^{iC_1}} \right\}, \quad (37)$$

$${}_1\bar{v}_\xi(\bar{x}, 0) = \frac{\bar{\kappa}^2}{4} e^{-i\bar{\omega}\bar{x}} \left\{ \sum_{m=1}^{m^+} e^{imC_2} \left[m\bar{s} \cos \bar{\theta} + \frac{B^2}{i\bar{\omega}} (e^{-i\bar{\omega}(\bar{x} - md_1)/B^2} - 1) \right] \right.$$

$$- \sum_{m=0}^{-m^-} e^{imC_1} \left[m\bar{s} \cos \bar{\theta} + \frac{B^2}{i\bar{\omega}} (e^{-i\bar{\omega}(\bar{x} + md_2)/B^2} - 1) \right] H(-x) \quad (38)$$

$$\left. + \bar{s} \cos \bar{\theta} \frac{e^{iC_1}}{(1 - e^{iC_1})^2} + \frac{B^2}{i\bar{\omega}} \left[\frac{e^{-i\bar{\omega}\bar{x}/B^2}}{(1 - e^{iC_6})} - \frac{1}{(1 - e^{iC_1})} \right] \right\}.$$

where $C_1 = -\bar{\omega}\bar{s} \sin \bar{\theta} - \bar{\omega}\bar{s} \cos \bar{\theta}/B^2 - \phi$

$C_2 = +\bar{\omega}\bar{s} \sin \bar{\theta} - \bar{\omega}\bar{s} \cos \bar{\theta}/B^2 + \phi$

$C_6 = -\bar{\mu}\bar{s} \sin \bar{\theta} - \phi$

Turning now to the third term in equation (32), this is given by

$${}_2\bar{v}_\xi(\bar{x}, \bar{y}) = - \sum_{m=-\infty}^{+\infty} e^{-i\bar{\mu}(\bar{x} - m\bar{s} \sin \bar{\theta}) + im\phi} \frac{1}{4\pi^2} \int_{-\infty - \bar{\mu}}^{+\infty - \bar{\mu}} \frac{e^{-i\bar{\lambda}(\bar{x} - m\bar{s} \sin \bar{\theta})} d\bar{\lambda}}{(\bar{\lambda} + \bar{\omega}/B^2)} \int_{-\infty}^{+\infty} \frac{i\bar{\alpha}^2 \bar{\kappa}^4 e^{-i\bar{\alpha}(\bar{y} - m\bar{s} \cos \bar{\theta})} d\bar{\alpha}}{(\bar{\lambda}^2 - \bar{\alpha}^2)^2 (\bar{\lambda}^2 - \bar{\alpha}^2 - \bar{\kappa}^2)} \quad (39)$$

The summation over m will be transformed using a result given by Lighthill (1958), as Example 38 (pp. 67, 68). For a period of 2π , the result is

$$\frac{1}{2\pi} \sum_{m=-\infty}^{+\infty} e^{imx} = \sum_{\nu=-\infty}^{+\infty} \delta(x - 2\pi\nu) \quad (40)$$

This result is closely related to the Poisson summation formula. Applying this result to equation (39) gives

$${}_2\bar{v}_\xi(\bar{x}, \bar{y}) = -\frac{1}{2\pi} e^{-i\bar{\mu}\bar{x}} \sum_{\nu=-\infty}^{+\infty} \int_{-\infty - \bar{\mu}}^{+\infty - \bar{\mu}} \frac{e^{-i\bar{\lambda}\bar{x}} d\bar{\lambda}}{(\bar{\lambda} + \bar{\omega}/B^2)} \int_{-\infty}^{+\infty} e^{-i\bar{\alpha}\bar{y}} \delta(\bar{\mu}\bar{s} \sin \bar{\theta} + \bar{\lambda}\bar{s} \sin \bar{\theta} + \bar{\alpha}\bar{s} \cos \bar{\theta} + \phi - 2\pi\nu)$$

$$\times \left[\frac{i\bar{\alpha}^2}{(\bar{\lambda}^2 - \bar{\alpha}^2 - \bar{\kappa}^2)} - \frac{i\bar{\alpha}^2}{(\bar{\lambda}^2 - \bar{\alpha}^2)} - \frac{i\bar{\alpha}^2 \bar{\kappa}^2}{(\bar{\lambda}^2 - \bar{\alpha}^2)^2} \right] d\bar{\alpha} \quad (41)$$

Using the delta function to evaluate the integral over $\bar{\alpha}$ gives

$${}_2\bar{v}_\xi(\bar{x}, \bar{y}) = \frac{1}{2\pi i} e^{-i\bar{\mu}\bar{x} - iA\bar{y}} \frac{1}{\bar{s} \cos \bar{\theta}} \frac{1}{(\tan^2 \bar{\theta} - 1)} \sum_{\nu=-\infty}^{+\infty} \int_{-\infty - i\bar{\mu}}^{+\infty + i\bar{\mu}} e^{-i\bar{\lambda}(\bar{x} - \bar{y} \tan \bar{\theta})} d\bar{\lambda} \times \frac{(A - \bar{\lambda} \tan \bar{\theta})^2}{(\bar{\lambda} + \bar{\omega}/B^2)^2} \\ \times \left[\frac{1}{(\bar{\lambda} - \Omega^+)(\bar{\lambda} - \Omega^-)} - \frac{1}{(\bar{\lambda} - \Omega_p^+)(\bar{\lambda} - \Omega_p^-)} + \frac{\bar{\kappa}^2}{(\tan^2 \bar{\theta} - 1)(\bar{\lambda} - \Omega_p^+)^2(\bar{\lambda} - \Omega_p^-)^2} \right] \quad (42)$$

where

$$A = (-\bar{\mu}\bar{s} \sin \bar{\theta} - \phi + 2\pi\nu)/(\bar{s} \cos \bar{\theta}), \quad (43)$$

$$\Omega^\pm = A \frac{\tan \bar{\theta}}{\tan^2 \bar{\theta} - 1} \mp A \frac{1}{\tan^2 \bar{\theta} - 1} \left[1 - \frac{\bar{\kappa}^2}{A^2} (\tan^2 \bar{\theta} - 1) \right]^{1/2}, \quad (44)$$

$$\Omega_p^\pm = A \frac{\tan \bar{\theta}}{\tan^2 \bar{\theta} - 1} \mp A \frac{1}{\tan^2 \bar{\theta} - 1} = \frac{A}{\tan \bar{\theta} \pm 1}.$$

The terms in the square bracket in equation (42) correspond to the terms in the square bracket in equation (41). The first is the genuine unsteady cascade effect. The second and third terms are the quasi-steady effects which were added in equation (32) and are subtracted out again here.

In the evaluation of the integral over $\bar{\lambda}$, there are poles at $\bar{\lambda} = \Omega^+$ and $\bar{\lambda} = \Omega^-$, which correspond to pressure waves, and a pole at $\bar{\lambda} = -\bar{\omega}/B^2$, which corresponds to vorticity waves. There are also poles at $\bar{\lambda} = \Omega_p^+$ and $\bar{\lambda} = \Omega_p^-$ which are purely mathematical artifacts with no physical significance. For large values of $|\nu|$ or $|A|$, Ω^+ and Ω_p^+ coincide, and Ω^- and Ω_p^- coincide.

Due to the small negative imaginary part of $\bar{\omega}$, these poles are slightly displaced from the real axis in the $\bar{\lambda}$ plane. The positions are illustrated in Fig. 3, which also shows the contours used for the evaluation of the integral in equation (42), and the small displacement of the path of integration from the real axis will be noted. If the axial velocity is supersonic, all poles lie within the contour for a downstream point, and all effects are downstream. If the axial velocity is subsonic, which is the case illustrated in Fig. 3, the poles Ω^- and Ω_p^- lie within the contour used for an upstream point, so that these poles correspond to upstream going waves. The poles Ω^+ , Ω_p^+ , and $(-\bar{\omega}/B^2)$ lie within the contour used for a downstream point, so that these poles correspond to downstream going waves. Carrying out the contour integration yields

$${}_2\bar{v}_\xi(\bar{x}, \bar{y}) = 0, \quad \text{for } (\bar{x} - \bar{y} \tan \bar{\theta}) < 0, \quad (45) \\ = \sum_{\nu} (-J^+ - J^- - J^w + J_p^+ + J_p^- + J_p^w - J_q^+ - J_q^- - J_q^w),$$

for

$$(\bar{x} - \bar{y} \tan \bar{\theta}) > 0,$$

if the axial velocity is supersonic.

If the axial velocity is subsonic

$${}_2\bar{v}_\xi(\bar{x}, \bar{y}) = \sum_{\nu} (J^- - J_p^- + J_q^-), \quad \text{for } (\bar{x} - \bar{y} \tan \bar{\theta}) < 0, \quad (46) \\ = \sum_{\nu} (-J^+ - J^w + J_p^+ + J_p^w - J_q^+ - J_q^w), \quad \text{for } (\bar{x} - \bar{y} \tan \bar{\theta}) > 0$$

In these expressions

$$J^\pm = -C_3 \frac{(A - \Omega^\pm \tan \bar{\theta})^2}{(\Omega^\pm - \Omega^\mp)(\Omega^\pm + \bar{\omega}/B^2)} e^{-i\bar{x}(\Omega^\pm + \bar{\mu}) + i\bar{y}(\Omega^\pm \tan \bar{\theta} - A)}, \\ J_p^\pm = -C_3 \frac{(A - \Omega_p^\pm \tan \bar{\theta})^2}{(\Omega_p^\pm - \Omega_p^\mp)(\Omega_p^\pm + \bar{\omega}/B^2)} e^{-i\bar{x}(\Omega_p^\pm + \bar{\mu}) + i\bar{y}(\Omega_p^\pm \tan \bar{\theta} - A)}, \\ J^w = -C_3 \frac{(A + \bar{\omega} \tan \bar{\theta}/B^2)^2}{(-\bar{\omega}/B^2 - \Omega^+)(-\bar{\omega}/B^2 - \Omega^-)} e^{-i\bar{x}(-\bar{\omega}/B^2 + \bar{\mu}) + i\bar{y}(-\bar{\omega} \tan \bar{\theta}/B^2 - A)}, \\ J_p^w = -C_3 \frac{(A + \bar{\omega} \tan \bar{\theta}/B^2)^2}{(-\bar{\omega}/B^2 - \Omega_p^+)(-\bar{\omega}/B^2 - \Omega_p^-)} e^{-i\bar{x}(-\bar{\omega}/B^2 + \bar{\mu}) + i\bar{y}(-\bar{\omega} \tan \bar{\theta}/B^2 - A)}, \quad (47)$$

$$J_q^\pm = -C_3 \frac{\bar{\kappa}^2}{(\tan \bar{\theta} - 1)} \left\{ \frac{2 \tan \bar{\theta} (A - \Omega_p^\pm \tan \bar{\theta})}{(\Omega_p^\pm - \Omega_p^\mp)^2 (\Omega_p^\pm + \bar{\omega}/B^2)} - \frac{2(A - \Omega_p^\pm \tan \bar{\theta})}{(\Omega_p^\pm - \Omega_p^\mp)^3 (\Omega_p^\pm + \bar{\omega}/B^2)} \right. \\ \left. - \frac{(A - \Omega_p^\pm \tan \bar{\theta})^2}{(\Omega_p^\pm - \Omega_p^\mp)^2 (\Omega_p^\pm + \bar{\omega}/B^2)^2} - \frac{i(\bar{x} - \bar{y} \tan \bar{\theta})(A - \Omega_p^\pm \tan \bar{\theta})^2}{(\Omega_p^\pm - \Omega_p^\mp)^2 (\Omega_p^\pm + \bar{\omega}/B^2)} \right\} e^{-i\bar{x}(\Omega_p^\pm + \bar{\mu}) + i\bar{y}(\Omega_p^\pm \tan \bar{\theta} - A)},$$

$$J_q^w = -C_3 \frac{\bar{\kappa}^2}{(\tan^2 \bar{\theta} - 1)} \frac{(A + \bar{\omega} \tan \bar{\theta}/B^2)^2}{(-\bar{\omega}/B^2 - \Omega_p^+)^2 (-\bar{\omega}/B^2 - \Omega_p^-)^2} e^{-i\bar{x}(-\bar{\omega}/B^2 + \bar{\mu}) + i\bar{y}(-\bar{\omega} \tan \bar{\theta}/B^2 - A)}$$

where

$$C_3 = \frac{1}{\bar{s} \cos \bar{\theta} (\tan^2 \bar{\theta} - 1)}.$$

When the axial velocity is supersonic the argument of the square root in equation (44) is always positive, and the disturbances take the form of waves propagating away from the row of dipoles. But when the axial velocity is subsonic the argument may become negative, Ω^+ and Ω^- become complex, and the pressure disturbances decay exponentially with distance from the row. The marginal condition is

$$1 - \frac{\bar{\kappa}^2}{A^2} (\tan^2 \bar{\theta} - 1) = 0. \quad (48)$$

This is the 'resonance' or 'cut-off' condition, and corresponds to waves carrying energy in a direction parallel to the cascade direction. The corresponding expression for the phase angle is

$$\phi - 2\pi\nu = \{-M \tan \bar{\theta} \pm (\tan^2 \bar{\theta} - 1)^{1/2}\} \bar{\kappa} \bar{s} \cos \bar{\theta}. \quad (49)$$

At this resonance condition, $\Omega^+ = \Omega^-$ and J^+ and J^- become infinite. The calculation therefore fails at these two points, and discontinuities in the results are to be expected.

Equations (47) show that there are three other points at which some of the J functions become infinite. These are at $(\Omega_p^+ + \bar{\omega}/B^2) = 0$, $(\Omega_p^- + \bar{\omega}/B^2) = 0$, and $\Omega_p^+ = \Omega_p^-$ (corresponding to $A = 0$). The calculation also fails at these three points, but this is purely a result of the mathematical devices used, and has no physical significance. The further possibility, $(\Omega^\pm + \bar{\omega}/B^2) = 0$, never occurs.

The series over ν for J^\pm , J_p^\pm and J_q^\pm are evaluated numerically. The series for J^\pm alone is not uniformly convergent, since the terms do not decrease with increasing ν . The terms of zero order are removed by J_p^\pm and the terms of order ν^{-1} are removed by J_q^\pm . This leaves a series with terms of order ν^{-2} , which is good for numerical computation. This is the whole point of introducing the ${}_0\bar{v}_\xi$ and ${}_1\bar{v}_\xi$ terms in equation (32).

The series for J^w , J_p^w and J_q^w , which correspond to the vorticity waves, may be evaluated analytically. This will be done for the case $\bar{y} = 0$ and the required formulae are

$$\sum_{\nu=-\infty}^{+\infty} \frac{1}{(2\pi\nu - x)^2 - z^2} = \frac{i}{2z} \left[\frac{1}{1 - e^{i(z+x)}} + \frac{1}{1 - e^{i(z-x)}} - 1 \right], \\ \sum_{\nu=-\infty}^{+\infty} \frac{(2\pi\nu - x)^2}{\{(2\pi\nu - x)^2 - z^2\}^2} = \frac{i}{4z} \left[\frac{1}{1 - e^{i(z+x)}} + \frac{1}{1 - e^{i(z-x)}} - 1 \right] - \frac{1}{4} \left[\frac{1}{\{1 - e^{i(z+x)}\}^2} + \frac{1}{\{1 - e^{i(z-x)}\}^2} \right].$$

When the result is combined with equation (37) and (38), the final result for the kernel function in the case of subsonic axial velocity is as follows:

$$\bar{v}_\xi(\bar{x}, 0) = -\frac{1}{2} \sum_{m=1}^{+\infty} e^{im(-\bar{\mu}\bar{s} \cos \bar{\theta} - \phi)} \delta(\bar{x} + md_2) \\ - e^{-i\bar{\omega}\bar{x}} \left\{ - \sum_{m=1}^{-m-} e^{imC_1} \left(\frac{i\bar{\omega}}{4} \frac{1-B^2}{B^2} - m \frac{\bar{\kappa}^2}{4} \bar{s} \cos \bar{\theta} \right) + \frac{i\bar{\omega}}{4} \frac{1-B^2}{B^2} \frac{e^{iC_1}}{1 - e^{iC_1}} - \frac{\bar{\kappa}^2}{4} \bar{s} \cos \bar{\theta} \frac{e^{iC_1}}{(1 - e^{iC_1})^2} \right\} \\ - e^{-i\bar{\mu}\bar{x}} \left\{ \frac{i\bar{\omega}}{4} \frac{1+B^2}{B^2} \left(- \sum_{m=1}^{-m-} e^{imC_6} + \frac{e^{iC_6}}{1 - e^{iC_6}} \right) \right\} + \sum_{\nu=-\infty}^{+\infty} (J^- - J_p^- + J_q^-), \quad (50)$$

for $\bar{x} < 0$,

$$\bar{v}_\xi(\bar{x}, 0) = -\frac{1}{2} \sum_{m=0}^{+\infty} e^{im(-\bar{\mu}\bar{s} \cos \bar{\theta} + \phi)} \delta(\bar{x} - md_1) - e^{-i\bar{\omega}\bar{x}} \left\{ + \sum_{m=1}^{m+} e^{imC_2} \left(\frac{i\bar{\omega}}{4} \frac{1-B^2}{B^2} - m \frac{\bar{\kappa}^2}{4} \bar{s} \cos \bar{\theta} \right) \right. \\ \left. - \frac{i\bar{\omega}}{4} \frac{1-B^2}{B^2} \frac{e^{iC_2}}{1 - e^{iC_2}} + \frac{\bar{\kappa}^2}{4} \bar{s} \cos \bar{\theta} \frac{e^{iC_2}}{(1 - e^{iC_2})^2} + \frac{\bar{\omega}}{2B} \frac{\sinh(\bar{\omega}\bar{s} \cos \bar{\theta}/B)}{\cosh(\bar{\omega}\bar{s} \cos \bar{\theta}/B) - \cos(\phi + \bar{\omega}\bar{s} \sin \bar{\theta})} \right\} \\ - e^{-i\bar{\mu}\bar{x}} \left\{ \frac{i\bar{\omega}}{4} \frac{1+B^2}{B^2} \left(+ \sum_{m=1}^{m+} e^{-imC_6} + \frac{1}{1 - e^{iC_6}} \right) \right\} - \sum_{\nu} (J^+ - J_p^+ + J_q^+), \quad \text{for } \bar{x} \geq 0. \quad (51)$$

For the supersonic axial velocity case, there is no effect for $\bar{x} < 0$ (upstream of row of dipoles) and for $\bar{x} \geq 0$;

$$\begin{aligned}
\bar{v}_\xi(\bar{x}, 0) = & -\frac{1}{2} \sum_{m=0}^{+\infty} e^{im(-\bar{\mu}\bar{s} \cos \bar{\theta} + \phi)} \delta(\bar{x} - m d_1) - \frac{1}{2} \sum_{m=1}^{+\infty} e^{im(-\bar{\mu}\bar{s} \cos \bar{\theta} - \phi)} \delta(\bar{x} + m d_2) \\
& - e^{-i\bar{\omega}\bar{x}} \left\{ \sum_{m=1}^{-m-} e^{imC_1} \left(\frac{i\bar{\omega}}{4} \frac{1-B^2}{B^2} - m \frac{\bar{\kappa}^2}{4} \bar{s} \cos \bar{\theta} \right) + \sum_{m=1}^{m+} e^{imC_2} \left(\frac{i\bar{\omega}}{4} \frac{1-B^2}{B^2} - m \frac{\bar{\kappa}^2}{4} \bar{s} \cos \bar{\theta} \right) \right. \\
& - \frac{i\bar{\omega}}{4} \frac{1-B^2}{B^2} \left(\frac{e^{iC_1}}{1-e^{iC_1}} + \frac{e^{iC_2}}{1-e^{iC_2}} \right) + \frac{\bar{\kappa}^2}{4} \bar{s} \cos \bar{\theta} \left[\frac{e^{iC_1}}{(1-e^{iC_1})^2} + \frac{e^{iC_2}}{(1-e^{iC_2})^2} \right] \\
& \left. + \frac{\bar{\omega}}{2B} \frac{\sinh(\bar{\omega}\bar{s} \cos \bar{\theta}/B)}{\cosh(\bar{\omega}\bar{s} \cos \bar{\theta}/B) - \cos(\phi + \bar{\omega}\bar{s} \sin \bar{\theta})} \right\} \\
& + e^{-i\bar{\mu}\bar{x}} \frac{i\bar{\omega}}{4} \frac{1+B^2}{B^2} \left\{ \sum_{m=1}^{m-} e^{imC_6} + \sum_{m=1}^{m+} e^{-imC_6} + 1 \right\} - \sum_{\nu=-\infty}^{+\infty} (J^- - J_p^- + J_q^- + J^+ - J_p^+ + J_q^+). \tag{52}
\end{aligned}$$

4. Effect of Wave Reflections

The integral equation which has to be solved is, from equations (11) and (27)

$$\int_{-1/2}^{+1/2} \bar{f}(\bar{\xi}) \bar{v}_\xi(\bar{x} - \bar{\xi}, 0) d\bar{\xi} = \bar{v}_U \tag{53}$$

where \bar{v}_ξ is the known kernel function from equations (50), (51) and (52), and \bar{v}_U is the known upwash velocity.

In the general unsteady case, this equation has to be solved numerically, $\bar{f}(\bar{\xi})$ being specified at N points evenly distributed along the chord. The integral equation is then replaced by a set of N simultaneous linear equations. In its simplest form this scheme was found to be very inaccurate. The reason may be seen by noting that the leading term in the kernel function is the sum of a number of delta functions, and that in the steady case ($\bar{\omega} = 0$) this is the only term. This term corresponds physically to the Mach waves radiating from the row of dipoles on other blades hitting the reference blade, as shown in Fig. 2. When these Mach waves hit another blade, they ought to be reflected. In the numerical scheme, the wave originating at one of the points where $\bar{f}(\bar{\xi})$ is specified on one of the other blades will not hit the reference blade exactly at a point where $\bar{f}(\bar{\xi})$ is specified, and the reflection is very imperfectly modelled by the numerical scheme. This is the cause of the inaccuracy, and it occurs whatever numerical interpolation scheme is used.

In order to overcome the difficulty, the reflections are allowed for explicitly. A new dipole strength, $\bar{g}(\bar{\xi})$, is defined along the chord of the reference blade, and with it go the additional dipole strengths necessary to give the required reflections. The total dipole strength, $\bar{f}(\bar{\xi})$, is therefore given by

$$\bar{f}(\bar{\xi}) = \bar{g}(\bar{\xi}) + \sum_{\text{reflections}} F_\alpha [\bar{g}(\bar{\xi} + d_p)]_{\xi_1}^{\xi_2}, \tag{54}$$

where F_α is a constant factor which depends on the phase angle between blades, d_p is a displacement distance, and the notation $[\]_{\xi_1}^{\xi_2}$ indicates that the term is to be included if $\xi_1 < \xi < \xi_2$. F_α , d_p , ξ_1 , and ξ_2 are given in Table 1 for various cases; and the corresponding wave reflection patterns are shown in Fig. 4.

Considering first the subsonic axial velocity case, if $d_2 > 1$ the wave from the trailing edge of one blade goes ahead of the blade above it, as shown in Fig. 4a, and there are no reflections. In steady flow there is no interference between blades, but in unsteady flow each blade can influence the flow over the blades behind it. If $d_2 < 1$ and $d_1 > 1$, the upward starting wave may be reflected once, as shown in Fig. 4b, but as the downward starting wave from the leading edge of one blade falls behind the trailing edge of the blade below it, the downward starting wave is never reflected. If $d_1 < 1$ and $(2d_1 - d_2) > 1$ the pattern is shown in Fig. 4c, with the upward starting wave reflected 0, 1 or 3 times, and the downward starting wave reflected 0 or 2 times. This is the usual design case for a fan tip section. If $(2d_1 - d_2) < 1$, there are possibilities of further reflections, as shown in Fig. 4d, but these cases are not thought to be of much practical importance.

If the axial velocity is supersonic, d_2 is negative, and if $(-d_2) > 1$ the waves from the leading edge of one blade go behind all other blades, as shown in Fig. 4e. There is then no interference between blades in steady or unsteady flow, and each blade behaves as an isolated aerofoil. Figs. 4f, 4g, and 4h show cases of increasing numbers of possible reflections.

When equation (54) is substituted into (53), the result may be written

$$\int_{-1/2}^{+1/2} \bar{g}(\bar{\xi}) \left\{ \bar{v}_{\xi}(\bar{x} - \bar{\xi}, 0) + \sum_{\text{reflections}} \left[F_a \bar{v}_{\xi}(\bar{x} - \bar{\xi} + d_p, 0) \right]_{\xi_1+d_p}^{\xi_2+d_p} \right\} d\bar{\xi} = \bar{v}_U. \quad (55)$$

This is the required integral equation for the unknown dipole strength $\bar{g}(\bar{\xi})$. When the kernel function, shown in braces thus $\{ \}$, is evaluated, all the delta functions cancel except for that at $(\bar{x} - \bar{\xi}) = 0$. The result is that $\bar{g}(\bar{\xi})$ is a smooth function of $\bar{\xi}$ over the range $-0.5 < \bar{\xi} < 0.5$, whereas $\bar{f}(\bar{\xi})$ shows discontinuities at the points where the waves from the leading and trailing edges of other blades are reflected.

The corresponding expressions for lift and moment are, from equations (15) and (16)

$$\bar{L} = \frac{L}{\pi \rho_0 U^2 c} = \frac{1}{\pi} \int_{-1/2}^{+1/2} \bar{g}(\bar{\xi}) \left\{ 1 + \sum_{\text{reflections}} [F_a]_{\xi_1+d_p}^{\xi_2+d_p} \right\} d\bar{\xi} \quad (56)$$

$$\bar{M}_\alpha = \frac{M_\alpha}{\pi \rho_0 U^2 c^2} = \frac{1}{\pi} \int_{-1/2}^{+1/2} \bar{g}(\bar{\xi}) \left\{ (\bar{\xi} - \bar{x}_n) + \sum_{\text{reflections}} [(\bar{\xi} - d_p - \bar{x}_n) F_a]_{\xi_1+d_p}^{\xi_2+d_p} \right\} d\bar{\xi}. \quad (57)$$

5. Numerical Solutions of Integral Equations

The dipole strength $\bar{g}(\bar{\xi})$ is specified at N equally spaced points along the chord of the reference blade given by

$$\bar{\xi} = -0.5 + \frac{I-1}{N-1}, \quad \text{for } 1 \leq I \leq N. \quad (58)$$

The upwash velocity is matched at the same points. Equations (12), (13) and (14) may therefore be written

$$V = \left[\frac{1}{B}, \frac{1}{B} + \frac{i\bar{\omega}}{B} (\bar{x} - \bar{x}_n), \frac{1}{B} e^{-i\bar{\omega}\bar{x}} \right] \begin{bmatrix} q/U \\ \alpha \\ w/U \end{bmatrix} = R \begin{bmatrix} q/U \\ \alpha \\ w/U \end{bmatrix}, \quad (59)$$

where R is a matrix with N rows (corresponding to the N matching points) and 3 columns (corresponding to the 3 kinds of upwash velocity).

The integrals in equations (55), (56) and (57) are evaluated by the trapezoidal rule; that is assuming that the integral varies linearly between the points given by equation (58). Equation (55) then gives

$$KG = V, \quad (60)$$

where G is a column matrix giving the values of the \bar{g} function, and K is a square $N \times N$ matrix giving the values of the kernel function.

Equations (56) and (57) may be written

$$\begin{bmatrix} \bar{L} \\ \bar{M}_\alpha \end{bmatrix} = AG \quad (61)$$

where A is a matrix with two rows and N columns, giving the coefficients necessary to evaluate the integrals.

Equations (59), (60) and (61) then give

$$\begin{bmatrix} \bar{L} \\ \bar{M}_\alpha \end{bmatrix} = C \begin{bmatrix} q/U \\ \alpha \\ w/U \end{bmatrix}, \quad (62)$$

where

$$C = \begin{bmatrix} C_{Lq} & C_{L\alpha} & C_{Lw} \\ C_{Mq} & C_{M\alpha} & C_{Mw} \end{bmatrix} = AK^{-1}R. \quad (63)$$

Two computer programs have been written in Fortran to calculate the force and moment coefficients given by equation (63). The first program works for both subsonic and supersonic axial velocity, but does not include C_{Lw} and C_{Mw} . The second program only covers the case of subsonic axial velocity, but since more care has been taken to optimise the coding it is much faster. On an IBM 370 this second program requires 64 K bytes of core store, and with $N = 16$ the execution time is about 0.3 seconds for each case.

6. Steady Solutions

The steady solution is obtained by putting $\bar{\omega} = 0$. Then equations (50) and (51) give (for $\phi \neq 2\pi n$)

$$\begin{aligned}\bar{v}_{\xi}(\bar{x}, 0) &= -\frac{1}{2} \sum_{m=1}^{\infty} e^{-im\phi} \delta(\bar{x} + md_2), \quad \bar{x} < 0, \\ \bar{v}_{\xi}(\bar{x}, 0) &= -\frac{1}{2} \sum_{m=0}^{\infty} e^{+im\phi} \delta(\bar{x} - md_1), \quad \bar{x} \geq 0.\end{aligned}$$

The kernel function of equation (55) then reduces to

$$K(\bar{x}) = -\frac{1}{2}\delta(\bar{x}). \quad (64)$$

In this case all three kinds of upwash velocity become identical, so that

$$R = \frac{1}{B}[1, 1, 1]. \quad (65)$$

The solution of equation (55) is therefore simply

$$\bar{g}(\bar{\xi}) = -\frac{2}{B}. \quad (66)$$

The force and moment coefficients are the same for all three kinds of upwash, so that

$$\begin{aligned}C_{Lq} &= C_{L\alpha} = C_{Lw} (= C_L), \\ C_{Mq} &= C_{M\alpha} = C_{Mw} (= C_M).\end{aligned} \quad (67)$$

In case (a) (subsonic axial velocity with no interference) the results are

$$\begin{aligned}\bar{f}(\bar{\xi}) &= -2/B, \\ C_L &= -2/\pi B, \\ C_M &= +2x_{\eta}/\pi B.\end{aligned} \quad (68)$$

In case (b) (subsonic axial velocity with one reflection of the upward starting wave) the results are

$$\begin{aligned}\bar{f}(\bar{\xi}) &= \begin{cases} -2(1 - e^{-i\phi})/B, & -0.5 < \bar{\xi} < (0.5 - d_2), \\ -2/B, & (0.5 - d_2) < \bar{\xi} < 0.5. \end{cases} \\ C_L &= -\frac{2}{\pi B}\{1 - e^{-i\phi}(1 - d_2)\}, \\ C_M &= +\frac{2}{\pi B}\{x_{\eta} - e^{-i\phi}(1 - d_2)(x_{\eta} + \frac{1}{2}d_2)\}.\end{aligned} \quad (69)$$

In case (c) (with up to three reflections of the upward starting wave and up to two reflections of the downward starting wave) the results are

$$\begin{aligned}\bar{f}(\bar{\xi}) &= -\frac{2}{B}\{1 - [e^{-i\phi}]_{-0.5-d_2}^{0.5-d_2} + [1 - e^{-i\phi}]_{-0.5+d_1}^{0.5} + [1 - e^{-i\phi}]_{-0.5+d_1-d_2}^{0.5-d_2}\}, \\ C_L &= -\frac{2}{\pi B}\{1 - e^{-i\phi}(1 - d_2) + 2(1 - \cos \phi)(1 - d_1)\}, \\ C_M &= +\frac{2}{\pi B}\{x_{\eta} - e^{-i\phi}(1 - d_2)(x_{\eta} + \frac{1}{2}d_2) + 2(1 - \cos \phi)(1 - d_1)(x_{\eta} - \frac{1}{2}d_1 + \frac{1}{2}d_2) \\ &\quad + i \sin \phi(1 - d_1)d_2\}.\end{aligned} \quad (70)$$

General expressions for the force and moment coefficients are

$$\begin{aligned}
C_L &= -\frac{2}{\pi B} \left\{ 1 - e^{-i\phi} (1-d_2) H(1-d_2) + 2(1-\cos\phi) \sum_{r=1}^{\infty} (1-rd_1+rd_2-d_2) H(1-rd_1+rd_2-d_2) \right\}, \\
C_M &= -x_\eta C_L - \frac{1}{\pi B} \left\{ e^{-i\phi} d_2 (1-d_2) H(1-d_2) \right. \\
&\quad \left. + \sum_{r=1}^{\infty} 2[r(1-\cos\phi)(d_1-d_2) - id_2 \sin\phi] (1-rd_1+rd_2-d_2) H(1-rd_1+rd_2-d_2) \right\}.
\end{aligned} \tag{71}$$

In these expressions, the H functions switch on the various reflections as they appear in groups of four with decreasing values of the cascade spacing.

These results are not strictly valid when $\phi = 0$ (or a multiple of 2π) so that all blades move in phase. The results then depend on the way in which the limits $\bar{\omega} \rightarrow 0$ and $\phi \rightarrow 0$ are approached, and in particular on the ratio $\bar{\omega}/\phi$. Actuator disc theory should be used for this case. But the results for cases (b) and (c) do correspond to steady flow in a cascade, when a particular back pressure is applied. It is interesting to note that over the front part of the blade, $-0.5 < \bar{\xi} < (0.5 - d_2)$, $\bar{f}(\bar{\xi})$ is zero. There is then no wave coming from the leading edge of the blade, and the effective incidence is zero. This corresponds to the unique incidence condition given by Kantrowitz (1946)⁷. In case (a), on the other hand, it is possible for Mach waves to pass upwards through the cascade, and each blade operates as an isolated aerofoil, with incidence.

For the cases of supersonic axial velocity, equation (66) is still true. General expressions for the force and moment coefficients are

$$\begin{aligned}
C_L &= -\frac{2}{\pi B} \left\{ 1 + \sum_{r=1}^{\infty} \left[-e^{-i\phi} (1-rd_1+rd_2+d_1) H(1-rd_1+rd_2+d_1) \right. \right. \\
&\quad \left. \left. - e^{+i\phi} (1-rd_1+rd_2-d_2) H(1-rd_1+rd_2-d_2) + 2(1-rd_1+rd_2) H(1-rd_1+rd_2) \right] \right\} \\
C_M &= -x_\eta C_L - \frac{1}{\pi B} \sum_{r=1}^{\infty} \left[-e^{-i\phi} (-rd_1+rd_2+d_1)(1-rd_1+rd_2+d_1) H(1-rd_1+rd_2+d_1) \right. \\
&\quad \left. - e^{+i\phi} (-rd_1+rd_2-d_2)(1-rd_1+rd_2-d_2) H(1-rd_1+rd_2-d_2) \right. \\
&\quad \left. + 2(-rd_1+rd_2)(1-rd_1+rd_2) H(1-rd_1+rd_2) \right]
\end{aligned} \tag{72}$$

In these expressions, the H functions switch on the various reflections as they occur with decreasing values of d_1 and $-d_2$.

Equations (68), (69), and (70) agree with the results given by Kurosaka (1973)⁸ for the same cases. In the general case, the result for the lift coefficient in equation (71) also agrees, but there appear to be some discrepancies in the results for the moment coefficient.

7. Quasi-Steady Solution

An analytical solution can be obtained when $\bar{\omega} \rightarrow 0$, retaining only terms of zero and first order in $\bar{\omega}$. The zero order terms are those already given as the steady solution. It is again necessary to exclude the case $\phi \rightarrow 0$. Only the case of subsonic axial velocity will be treated.

The expression for the induced velocity may then be written

$$\begin{aligned}
\bar{v}_\xi(\bar{x}, 0) &= -\frac{1}{2} \delta(\bar{x}) + \frac{i\bar{\omega}}{2B^2} \left\{ \frac{1}{1-e^{i\phi}} - H(\bar{x}) \right\} \\
&\quad - \frac{1}{2} \sum_{m=1}^{\infty} e^{im(-\bar{\mu}\bar{s} \cos \bar{\delta} + \phi)} \left\{ \delta(\bar{x} - md_1) + \frac{i\bar{\omega}}{B^2} H(\bar{x} - md_1) \right\} \\
&\quad - \frac{1}{2} \sum_{m=1}^{\infty} e^{im(-\bar{\mu}\bar{s} \cos \bar{\delta} - \phi)} \left\{ \delta(-\bar{x} - md_2) - \frac{i\bar{\omega}}{B^2} H(-\bar{x} - md_2) \right\}.
\end{aligned} \tag{73}$$

The kernel function of equation (55) then reduces to

$$K(\bar{x} - \bar{\xi}) = -\frac{1}{2} \delta(\bar{x} - \bar{\xi}) + \frac{i\bar{\omega}}{2B^2} \left\{ \frac{1}{1 - e^{i\phi}} H(-\frac{1}{2} + d_2 - \bar{\xi}) - H(\bar{x} - \bar{\xi}) \right\}. \quad (74)$$

This shows that, as for the delta functions, most of the H functions cancel out. However, this cancellation is not exact for the general unsteady case, and shows that reflection is not exactly modelled by putting a dipole on the reflecting surface.

The solution of the integral equation (55) may then be sought in the form

$$\bar{g}(\bar{\xi}) = -\frac{2}{B} [1, 1, 1] + i\bar{\omega}(A_0 + A_1 \bar{\xi}),$$

which shows the steady solution plus two terms of first order in $\bar{\omega}$. When this is substituted into the integral equation, and terms of second and higher order in $\bar{\omega}$ are neglected, it is found that the equation may be satisfied and the constants A_0 and A_1 determined. The result may be written in the form

$$\bar{g}(\bar{\xi}) = G_0 + G_1 \bar{\xi}_1 \quad (75)$$

where

$$G_0 = -\frac{2}{B} [1, 1, 1] - \frac{2i\bar{\omega}}{B^3} \left(\frac{d_2}{1 - e^{i\phi}} - \frac{1}{2} \right) [1, 1, 1] + \frac{2i\bar{\omega}x_\eta}{B} [0, 1, 0], \quad (76)$$

$$G_1 = \frac{2i\bar{\omega}}{B^3} [1, 1, 1] + \frac{2i\bar{\omega}}{B} [0, -1, 1]. \quad (77)$$

This result is true for subsonic axial velocity with any number of reflections, except that in case (a) with no reflections ($d_2 > 1$) the d_2 in equation (76) must be replaced by unity.

The following results for the force and moment coefficients have been obtained.

In case (a) (subsonic axial velocity with no interference)

$$C_L = \frac{G_0}{\pi}, \quad (78)$$

$$C_M = -x_\eta C_L + \frac{1}{12\pi} G_1.$$

In case (b) (subsonic axial velocity with one reflection of the upward starting wave)

$$C_L = \frac{1}{\pi} \left\{ G_0 - e^{-i\phi} (1 - d_2) \left(G_0 + \frac{1}{2} G_1 d_2 \right) - \frac{2i\bar{\omega}M^2 \bar{s} \cos \bar{\theta}}{B^3} e^{-i\phi} (1 - d_2) [1, 1, 1] \right\},$$

$$C_M = -x_\eta C_L + \frac{G_0}{2\pi} e^{-i\phi} d_2 (1 - d_2) + \frac{G_1}{12\pi} \{ 1 - e^{-i\phi} (1 - 2d_2 - 2d_2^2) (1 - d_2) \}$$

$$+ \frac{i\bar{\omega}M^2 \bar{s} \cos \bar{\theta}}{\pi B^3} e^{-i\phi} d_2 (1 - d_2) [1, 1, 1]. \quad (79)$$

In case (c)

$$C_L = \frac{G_0}{\pi} \{ 1 - e^{-i\phi} (1 - d_2) + 2(1 - \cos \phi)(1 - d_1) \}$$

$$+ \frac{G_1}{2\pi} \{ -e^{-i\phi} d_2 (1 - d_2) - 2(1 - \cos \phi)(d_1 - d_2)(1 - d_1) + 2i \sin \phi d_2 (1 - d_1) \}$$

$$+ \frac{2i\bar{\omega}M^2 \bar{s} \cos \bar{\theta}}{\pi B^3} \left\{ -e^{-i\phi} (1 - d_2) + [4(1 - \cos \phi) + 2i \sin \phi](1 - d_1) \right\} [1, 1, 1]. \quad (80)$$

$$\begin{aligned}
C_M = & -x_n C_L + \frac{G_0}{2\pi} \{e^{-i\phi} d_2(1-d_2) - [e^{+i\phi} d_1 - 2(d_1-d_2) + e^{-i\phi}(d_1-2d_2)](1-d_1)\} \\
& + \frac{G_1}{12\pi} \{1 - e^{-i\phi}(1-2d_2-2d_2^2)(1-d_2) + 2(1-\cos\phi)(1-2d_1-2d_1^2)(1-d_1) \\
& - 12[d_1(d_1-2d_2) + e^{-i\phi}d_2(d_1-d_2)](1-d_1)\} \\
& + \frac{i\bar{\omega}M^2\bar{s}\cos\bar{\theta}}{\pi B^3} \{e^{-i\phi}d_2(1-d_2) - [e^{i\phi}d_1 - 4(d_1-d_2) + 3e^{-i\phi}(d_1-2d_2)](1-d_1)\}[1, 1, 1].
\end{aligned}$$

In equations (78), (79) and (80), the symbols C_L and C_M denote the first and second rows respectively of the matrix C used in equation (5.5).

For torsional vibration, the results in equations (78) and (79) have been shown to agree with those obtained by Kurosaka (1973), but the results in equations (80) appear to show some discrepancies. For bending vibration, since Kurosaka's theory is based on the displacement rather than the velocity of vibration, he only obtains results which are comparable to those obtained in section of this paper headed "Steady Solutions".

8. Results and Comparison with Other Work

The convergence of the second computer program has been assessed by running with increasing numbers of matching points (N) for two cascades. The results are shown in Table 2. It is clear that the values of the force and moment coefficients rapidly approach a limit. It is concluded from this that $N = 16$ is sufficient to ensure accurate results, and that $N = 11$ is often enough.

The results of the programs have been compared with those obtained by several other workers.

Gorelov (1966)⁴ gave results for the case of zero stagger and therefore supersonic axial velocity. The notation used compares as follows

Gorelov	M	k	τ	β	μ	$C_y^1\alpha$	$C_y^{11}\alpha$	$C_M^1\alpha$	$C_M^{11}\alpha$
N. & W.	M	$\bar{\omega}/2$	$1/s$	θ	$-\phi$	$-2\pi\mathcal{R}(C_{L\alpha})$	$-2\pi\mathcal{I}(C_{L\alpha})$	$-2\pi\mathcal{R}(C_{M\alpha})$	$-2\pi\mathcal{I}(C_{M\alpha})$

Figures 5 and 6 show a comparison between the results obtained, for the force and moment coefficients due to torsion. Very close agreement is seen.

Nishiyama and Kikuchi (1974)¹² gave results for the case of a staggered cascade with supersonic axial velocity. The notation used compares as follows

Nishiyama	M	K	$d/2b$	λ	τ	$(p_- - p_+)/(\frac{1}{2}\rho_\infty U_\infty^2)$
N. & W.	M	$\bar{\omega}/2$	s	θ	$-\phi$	$-2\bar{f}$

Fig. 7 shows the comparison for the pressure difference across the blade due to torsional vibration. Good agreement is seen. It will also be noted how, for this case of supersonic axial velocity, the pressure difference across the forward part of the blade is independent of phase angle. There is then a discontinuity at the point where the wave from the leading edge of the blade below hits the reference blade, and behind this point the pressure difference depends on phase angle.

Verdon and McCune (1975) have given rather complete results for two cascades with subsonic axial velocity. The notation used compares as follows

Verdon & McCune	M	k	s	θ	σ	$p^- - p^+$	C_M
N. & W.	M	$\bar{\omega}M/B^2$	c/s	θ	ϕ	$-2\bar{f}$	$2\pi C_{M\alpha}$

Figure 8 shows the pressure difference across the blade for 'Cascade A', which is the case when the downward starting wave from the leading edge of one blade passes behind the trailing edge of the blade below. There is then one discontinuity in the pressure distribution. Fig. 9 shows similar results for 'cascade B'. In this case there may be two reflections of the downward starting wave, and the pressure distributions show three discontinuities. Figs. 10 and 11 show results for the moment coefficient due to torsion. In all cases

the agreement between the two programs is very close. Figs. 10 and 11 also show discontinuities at the two "resonance" points. Between these points the Verdon and McCune program fails to converge.

Fig. 12 shows comparison with some results taken from the paper by Snyder and Commerford (1974)¹⁶ which were obtained using Verdon's (1973)¹⁷ earlier program for a finite cascade. This is less accurate than the later Verdon and McCune (1975)¹⁸ program, but it does give results for the range of phase angle between the resonance points. Good agreement is seen, except for points close to the resonance points.

Finally, Fig. 13 shows results which were obtained for comparison with an annular cascade experiment which has been reported by Whitehead, Watson, Nagashima, and Grant (1976)¹⁹. In this case only a few points have been computed in the region between the resonance points. So far the experimental results have not been extended to a sufficiently high Mach number to enable any significant comparison to be made between the experimental results and the theory presented here.

9. Conclusions

A theory has been presented for the calculation of unsteady linearised flow in supersonic cascades. Analytical results are given for the steady flow and quasi-steady flow limits. For the general unsteady flow case, the method leads to a fast computer program. In all cases good agreement with previous work has been obtained.

Single degree of freedom bending flutter would be predicted if the real part of the force coefficient C_{Lq} became positive. In fact it has always been found that this number is negative, so that bending vibration is always stable.

Single degree of freedom torsional flutter is predicted if the imaginary part of the moment coefficient C_{Mq} becomes positive. Figs. 6, 10, 11, 12 and 13 show extensive ranges of phase angle for which this condition is met, when the torsional axis is at the mid-chord point, so that extensive flutter of this kind is predicted.

In practice, transonic fan blades are coupled together at a point about three quarters of the way up the blade by snubbers, so that the principal modes of vibration include both bending and torsion. The present program can be used to predict flutter in a mode of this kind.

The program can also be used to predict the amplitude of vibration forced by wakes.

LIST OF SYMBOLS

The notation used is illustrated in Figure 1.

A	Equation (43).
a_0	Free stream sound speed.
B	$(M^2 - 1)^{\frac{1}{2}}$.
$C_{L\alpha}$	Force coefficient due to bending.
$C_{L\alpha}$	Force coefficient due to torsion.
C_{LW}	Force coefficient due to wakes.
$C_{M\alpha}$	Moment coefficient due to bending.
$C_{M\alpha}$	Moment coefficient due to torsion.
C_{MW}	Moment coefficient due to wakes.
C	Matrix of force and moment coefficients. Equation (63).
c	Chord.
d_1	$\bar{s}(\sin \bar{\theta} + \cos \bar{\theta})$. Displacement distance for downward wave.
d_2	$\bar{s}(\sin \bar{\theta} - \cos \bar{\theta})$. Displacement distance for upward wave.
d_p	Displacement distance for reflections.
F_α	Factor for reflections.
F	Generalized body force.
f	Lift distribution along chord.
\bar{f}	$f/\rho_0 U^2$.
G	Green's function.
\bar{g}	Lift distribution before allowing for reflections.
H	Heaviside step function.
I	Integer specifying point number along blade.
i	$(-1)^{\frac{1}{2}}$.
J	Bessel function. Also equations (47).
K	Kernel function.
L	Lift force.
\bar{L}	$L/\pi\rho_0 U^2 c$.
M	U/a_0 .
M_α	Moment, positive nose down.
\bar{M}_α	$M_\alpha/\pi\rho_0 U^2 c^2$.
m	Integer specifying blade.
N	Number of points used along chord.
p	Pressure.
\bar{p}	$p/\rho_0 U^2$.
q	Upward velocity of blade due to bending vibration.

R	Matrix, equation (59).
s	Blade spacing.
\bar{s}	$sB \cos \theta / c \cos \bar{\theta}$.
t	Time.
U	Free stream velocity.
u	Perturbation velocity, parallel to chord.
\bar{u}	u/U .
v	Perturbation velocity, perpendicular to chord.
\bar{v}	v/BU .
w	Velocity, perpendicular to chord, due to wakes.
x	Coordinate parallel to chord.
\bar{x}	x/c .
x_η	Torsional axis position.
y	Coordinate perpendicular to chord.
\bar{y}	yB/c .
α	Wave number in y direction.
$\bar{\alpha}$	$c\alpha/B$.
α_0	Torsional amplitude, positive nose down.
γ	Ratio of specific heats.
δ	Dirac delta function.
η	y coordinate for force distribution.
θ	Stagger angle.
$\bar{\theta}$	$\tan^{-1}(\tan \theta/B)$.
$\bar{\kappa}$	$\bar{\omega}M/B^2$.
λ	Wave number in x direction.
$\bar{\lambda}$	$c\lambda - \bar{\mu}$.
$\bar{\mu}$	$M\bar{\kappa} = \bar{\omega}M^2/B^2$.
ν	Integer specifying acoustic wave.
ξ	x coordinate for force distribution.
$\bar{\xi}$	ξ/c ,
ρ_0	Freestream density.
ρ	Perturbation density.
ϕ	Phase angle between blades.
Ω^\pm	Equation (44).
Ω_p^\pm	Equation (44).
ω	Angular frequency of vibration.
$\bar{\omega}$	$\omega c/U$, Frequency parameter.
$\frac{D}{Dt}$	$\frac{\partial}{\partial t} + U \frac{\partial}{\partial x}$.

$$\nabla^2 = \frac{\partial^2}{\partial x^2} + \frac{\partial^2}{\partial y^2}.$$

Other symbols used locally in the text are defined as they occur.

REFERENCES

- | <i>No.</i> | <i>Author(s)</i> | <i>Title</i> |
|------------|---|---|
| 1 | C. W. Brix, Jr. and M. F. Platzer . . . | Theoretical investigations of supersonic flow past oscillating cascades with subsonic leading-edge locus.
AIAA Paper No. 74-14 (1974). |
| 2 | D. G. Drake | The oscillating two-dimensional aerofoil between porous walls.
<i>Aero Quart.</i> , Vol. 8, p. 226 (1957). |
| 3 | M. E. Goldstein | Cascade with subsonic leading-edge locus.
<i>AIAA Journ.</i> , Vol. 13, p. 1117 (1975). |
| 4 | D. N. Gorelov | Cascade of plates in an unsteady supersonic flow.
<i>Mech. Zhid i Gaza</i> , Vol. 1, 1966, No. 4, p. 50.
<i>Trans. Fluid Dynamics</i> , Vol. 1, No. 4, p. 34 (1966). |
| 5 | D. G. Halliwell | The characteristics, prediction and test analysis of supersonic flutter in turbofan engines.
Proc. I. Mech. E. Conf. on 'Vibrations in Rotating Machinery',
Churchill College, Cambridge (Sept. 1976). |
| 6 | S. Kaji and T. Okazaki | Propagation of sound waves through a blade row. II Analysis based on the acceleration potential method.
<i>J. Sound Vib.</i> , Vol. 11, pp. 355-373 (1970). |
| 7 | A. Kantrowitz | The supersonic axial-flow compressor.
NACA Rep. 974 (1946). |
| 8 | M. Kurosaka | On the unsteady supersonic cascade with a subsonic leading edge. An exact first order theory. Parts I and II.
<i>Trans. ASME, A</i> , Vol. 96, p. 13 (1973). |
| 9 | F. Lane | Supersonic flow past an oscillating cascade with supersonic leading edge locus.
<i>J. Aero Sci.</i> , Vol. 24, p. 65 (1957). |
| 10 | J. W. Miles | The compressible flow past an oscillating airfoil in a wind tunnel.
<i>J. Aero Sci.</i> , Vol. 23, p. 671 (1956). |
| 11 | M. Namba | Lifting surface theory for unsteady flows in a rotating annular cascade.
<i>Revue Francaise de Mecanique</i> . Numero Special. (1976). p. 39, IUTAM.
Symposium on Aeroelasticity in Turbomachines, Paris (Oct. 1976). |
| 12 | T. Nishiyama and M. Kikuchi | Theoretical analysis for unsteady characteristics of oscillating aerofoils in supersonic flows.
Tech. Rep., Tohoku Univ., Vol. 38, No. 2 (1973). |
| 13 | M. F. Platzer, W. R. Chadwick and P. B. Schlein | On the analysis of the aerodynamic and flutter characteristics of transonic compressor blades.
<i>Revue Francaise de Mecanique</i> . Numero Special. (1976). p. 65, IUTAM.
Symposium on Aeroelasticity in Turbomachines, Paris (Oct. 1976). |

- 14 M. F. Platzer and H. G. Chalkley .. Theoretical investigations of supersonic cascade flutter and related interference problems.
AIAA Paper No. 72-377 (1972).
- 15 S. N. Smith Discrete frequency sound generation in axial flow turbomachines.
A.R.C. R. and M. 3709 (1972).
- 16 L. E. Snyder and G. L. Commerford Supersonic unstalled flutter in fan rotors; analytical and experimental results.
J. Engg. Power Trans. ASME, A. Vol. 76, pp. 379-386 (1974).
- 17 J. M. Verdon The unsteady aerodynamics of a finite supersonic cascade with subsonic axial velocity.
J. Ap. Mech. Trans. ASME, E, Vol. 40, pp. 667-671 (1973).
- 18 J. M. Verdon and J. E. McCune ... Unsteady supersonic cascade in subsonic axial flow.
AIAA Jour., Vol. 13, pp. 193-201 (1975).
- 19 D. S. Whitehead, P. J. Watson, T. Nagashima and R. J. Grant An experiment to measure moment coefficients for aerofoils oscillating in cascade.
Revue Francaise de Mecanique. Numero.Special. (1976) p. 123, IUTAM Symposium on Aeroelasticity in Turbomachines, Paris (Oct. 1976).

TABLE 1
Wave Reflection Factors

Subsonic axial velocity ($d_2 > 0$)					
Wave starting	Reflection No.	F_a	d_p	ξ_1	ξ_2
Upward	1	$-E_2$	d_2	-0.5	$+0.5 - d_2$
Downward	1	$-E_1$	$-d_1$	$-0.5 + d_1$	$+0.5$
Upward	2	$E_1 E_2$	$-d_1 + d_2$	$-0.5 + d_1$	$+0.5$
Downward	2	$E_1 E_2$	$-d_1 + d_2$	$-0.5 + d_1 - d_2$	$+0.5 - d_2$
Upward	3	$-E_1 E_2^2$	$-d_1 + 2d_2$	$-0.5 + d_1 - d_2$	$+0.5 - d_2$
Supersonic axial velocity ($d_2 < 0$)					
Wave starting	Reflection No.	F_a	d_p	ξ_1	ξ_2
Upward	1	$-E_2$	d_2	$-0.5 - d_2$	$+0.5$
Downward	1	$-E_1$	$-d_1$	$-0.5 + d_1$	$+0.5$
Upward	2	$E_1 E_2$	$-d_1 + d_2$	$-0.5 + d_1 - d_2$	$+0.5$
Downward	2	$E_1 E_2$	$-d_1 + d_2$	$-0.5 + d_1 - d_2$	$+0.5$
Upward	3	$-E_1 E_2^2$	$-d_1 + 2d_2$	$-0.5 + d_1 - 2d_2$	$+0.5$
Downward	3	$-E_1^2 E_2$	$-2d_1 + d_2$	$-0.5 + 2d_1 - d_2$	$+0.5$

$d_1 = \bar{s}(\sin \bar{\theta} + \cos \bar{\theta})$
 $d_2 = \bar{s}(\sin \bar{\theta} - \cos \bar{\theta})$
 $E_1 = \exp(-i\bar{\mu}\bar{s} \cos \bar{\theta} + i\phi)$
 $E_2 = \exp(-i\bar{\mu}\bar{s} \cos \bar{\theta} - i\phi)$

TABLE 2
Convergence of Supersonic Vibration Program

<i>Cascade 'A' 'k = 0.5'</i>							
$M = 1.3454, \quad \bar{\omega} = 0.3010, \quad s/c = 0.7889, \quad \theta = 59.53^\circ, \quad x_\eta = 0, \quad \phi = -30^\circ.$							
	<i>N</i>	6	10	11	16	21	26
C_{Lq}	<i>R</i>	-0.1574	-0.1593	-0.1580	-0.1592	-0.1589	-0.1593
	<i>I</i>	0.3812	0.3810	0.3831	0.3822	0.3827	0.3821
$C_{L\alpha}$	<i>R</i>	-0.1383	-0.1400	-0.1385	-0.1396	-0.1393	-0.1397
	<i>I</i>	0.3877	0.3882	0.3900	0.3894	0.3898	0.3893
C_{LW}	<i>R</i>	-0.1759	-0.1782	-0.1767	-0.1780	-0.1777	-0.1781
	<i>I</i>	0.3729	0.3721	0.3745	0.3733	0.3738	0.3731
C_{Mq}	<i>R</i>	-0.0245	-0.0245	-0.0238	-0.0241	-0.0240	-0.0242
	<i>I</i>	0.0613	0.0644	0.0639	0.0648	0.0648	0.0650
$C_{M\alpha}$	<i>R</i>	-0.0192	-0.0186	-0.0180	-0.0181	-0.0180	-0.0181
	<i>I</i>	0.0377	0.0412	0.0407	0.0417	0.0417	0.0420
C_{MW}	<i>R</i>	-0.0303	-0.0307	-0.0300	-0.0304	-0.0303	-0.0306
	<i>I</i>	0.0844	0.0871	0.0867	0.0874	0.0875	0.0877
<i>Cascade 'B' 'k = 2.0'</i>							
$M = 1.2806, \quad \bar{\omega} = 1.0, \quad s/c = 0.6708, \quad \theta = 63.43^\circ, \quad x_\eta = 0, \quad \phi = 0.$							
	<i>N</i>	6	10	11	16	21	26
C_{Lq}	<i>R</i>	-0.2233	-0.2280	-0.2266	-0.2291	-0.2290	-0.2292
	<i>I</i>	-0.0795	-0.0754	-0.0771	-0.0754	-0.0754	-0.0761
$C_{L\alpha}$	<i>R</i>	-0.1767	-0.1822	-0.1804	-0.1830	-0.1832	-0.1822
	<i>I</i>	-0.0816	-0.0788	-0.0806	-0.0787	-0.0789	-0.0795
C_{LW}	<i>R</i>	-0.2629	-0.2670	-0.2661	-0.2686	-0.2682	-0.2695
	<i>I</i>	-0.0724	-0.0682	-0.0698	-0.0683	-0.0683	-0.0691
C_{Mq}	<i>R</i>	0.0022	0.0013	0.0012	0.0042	0.0033	0.0035
	<i>I</i>	0.0433	0.0449	0.0440	0.0466	0.0457	0.0473
$C_{M\alpha}$	<i>R</i>	-0.0367	-0.0383	-0.0383	-0.0352	-0.0361	-0.0359
	<i>I</i>	-0.0211	-0.0177	-0.0193	-0.0163	-0.0171	-0.0155
C_{MW}	<i>R</i>	0.0391	0.0385	0.0386	0.0412	0.0404	0.0406
	<i>I</i>	0.1113	0.1106	0.1106	0.1125	0.1115	0.1131

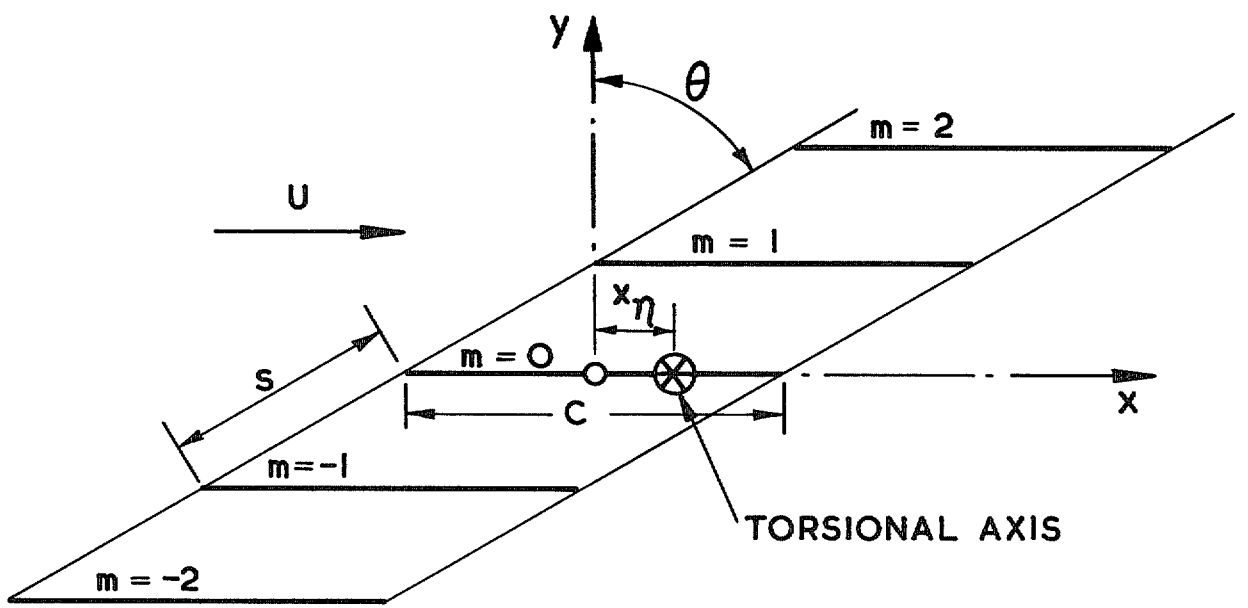


FIG. 1. Notation.

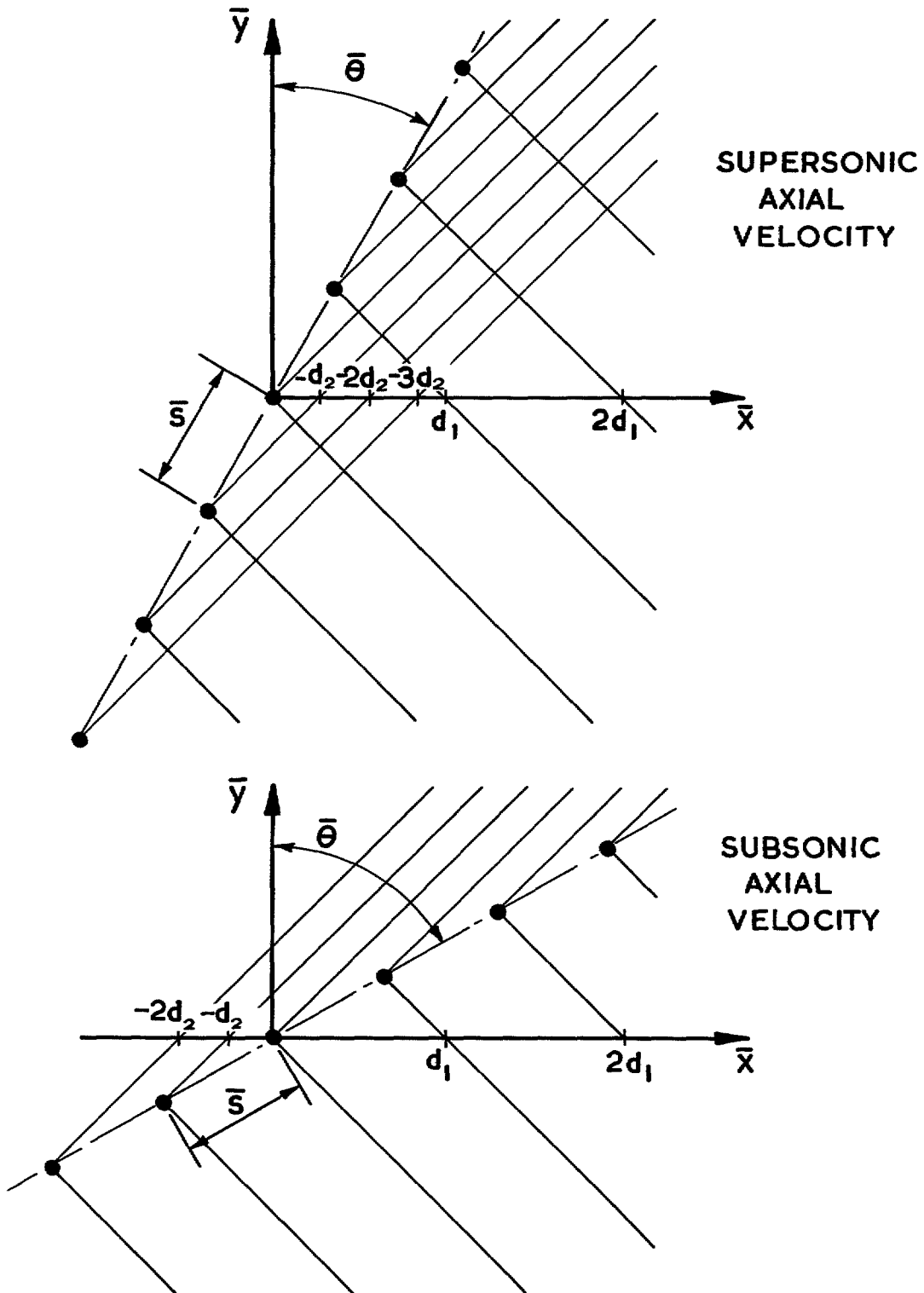


FIG. 2. Wave patterns in transformed plane.

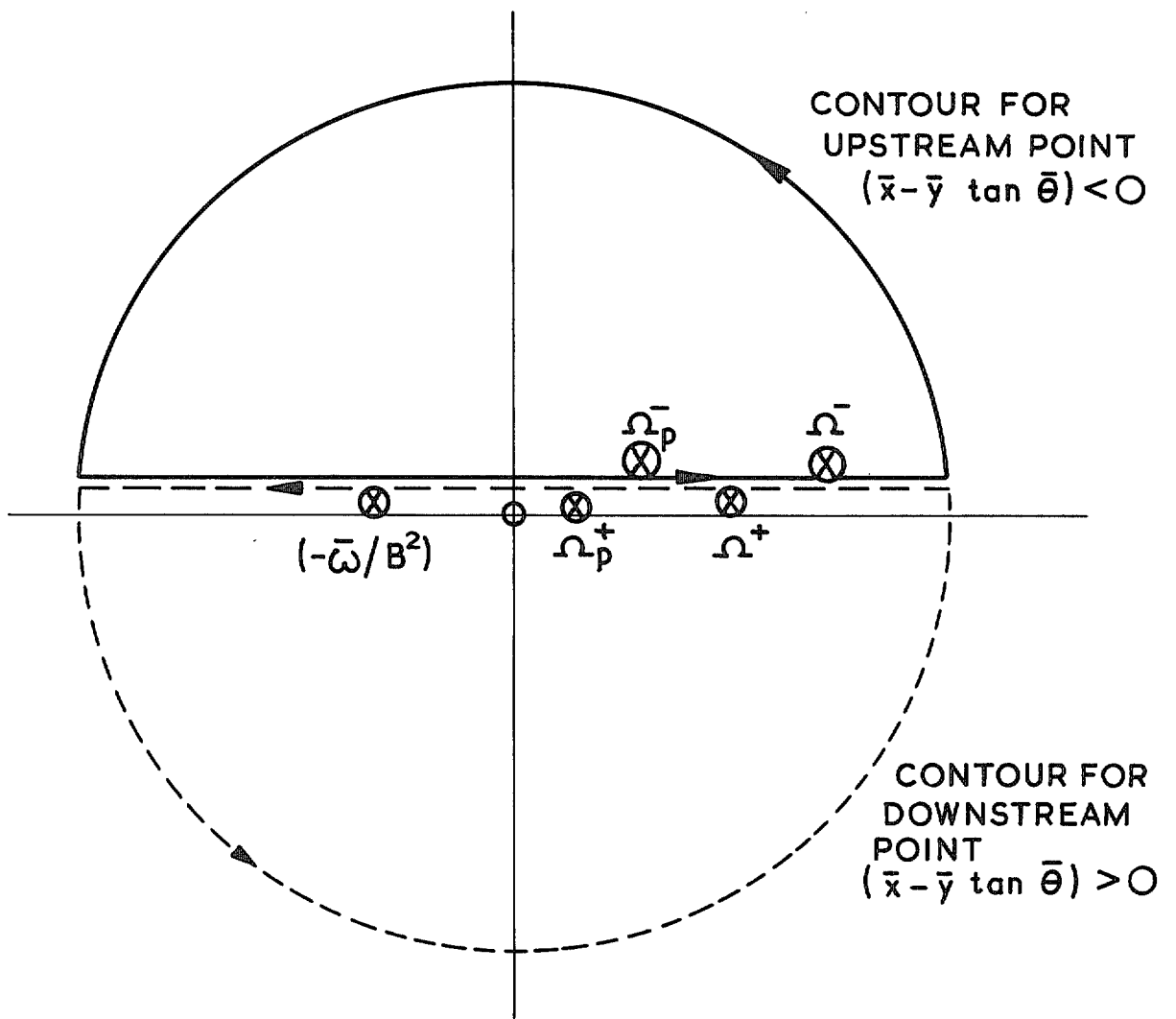


FIG. 3. Position of poles in λ plane; subsonic axial velocity case.

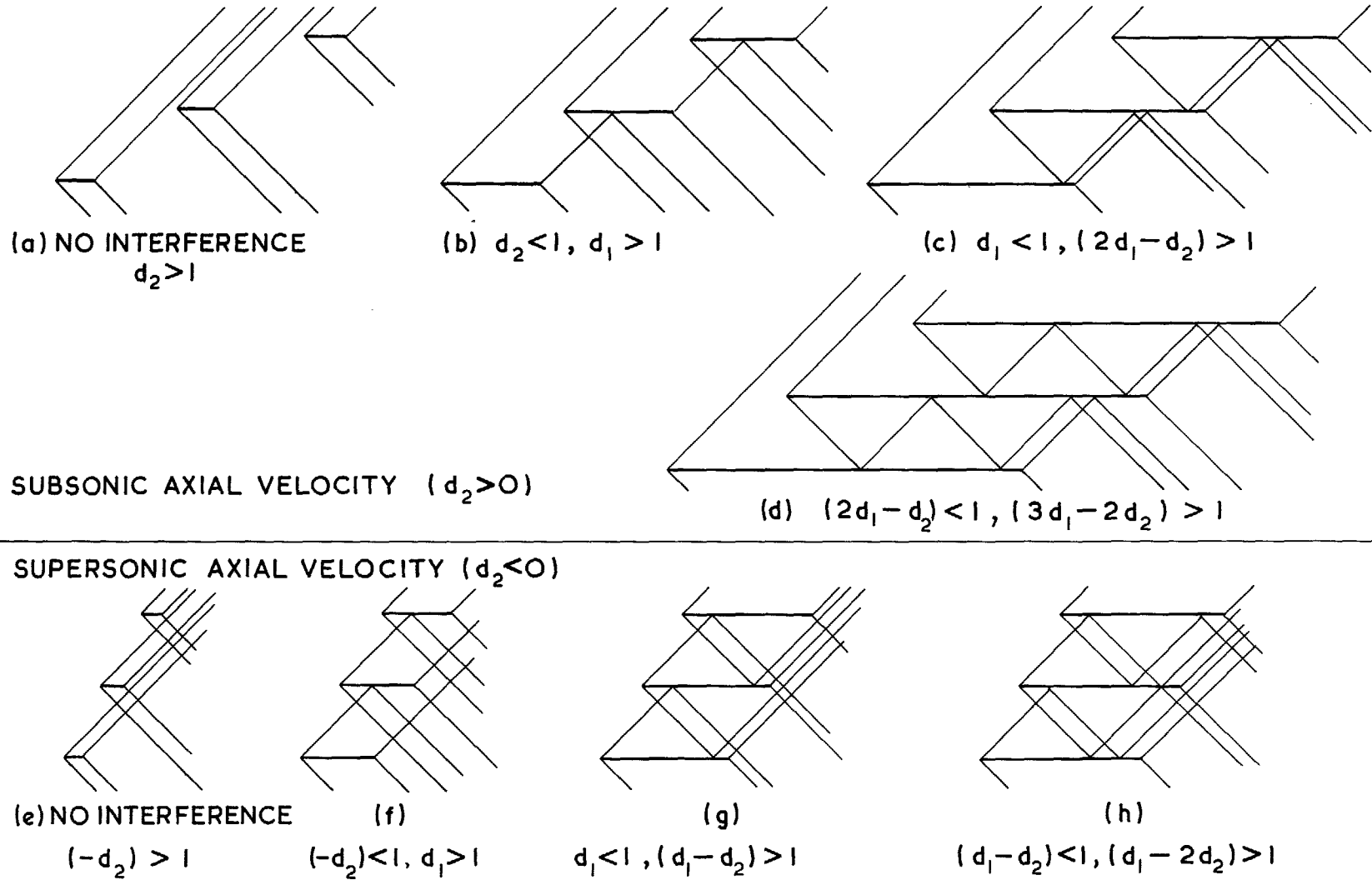


FIG. 4. Wave reflection patterns.

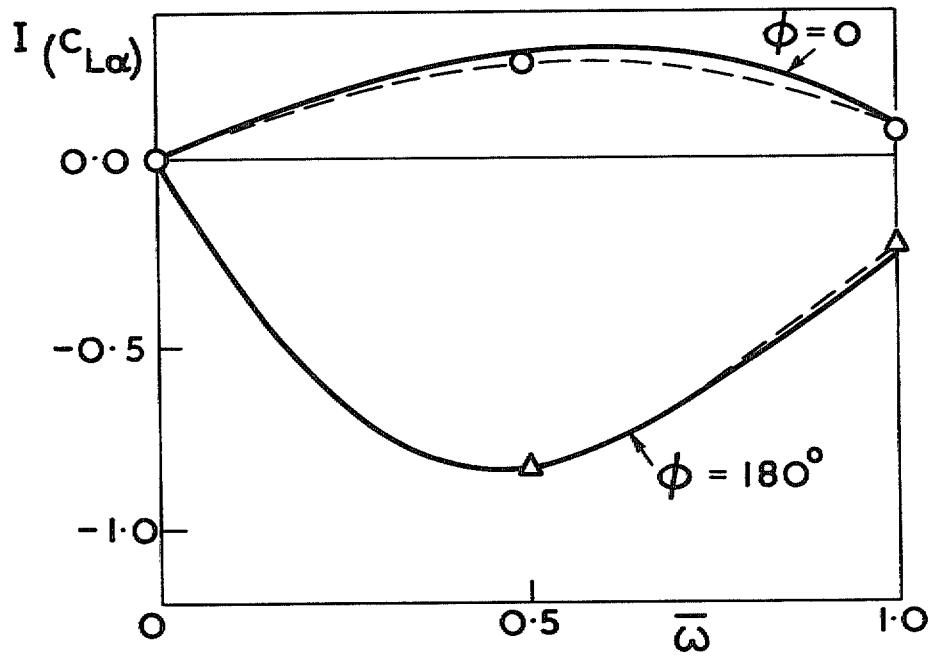
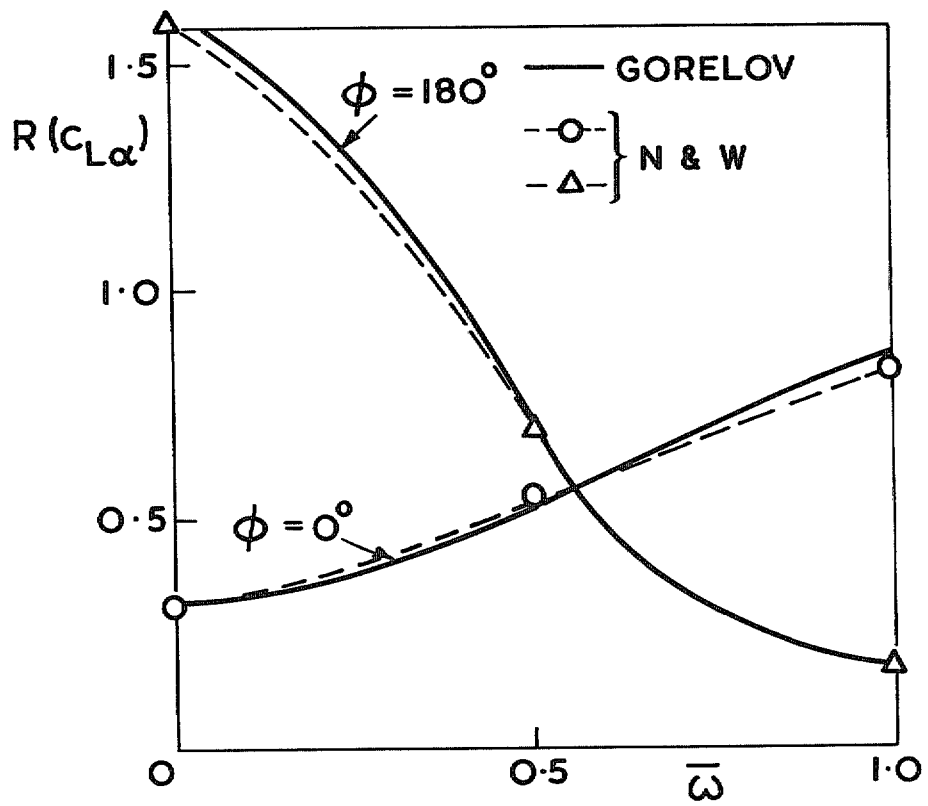


FIG. 5. Comparison with Gorelov; force coefficient due to torsion. $M = 1.2$, $s/c = 1.0$, $\theta = 0^\circ$, $x_\eta = 0.0$, $N = 21$.

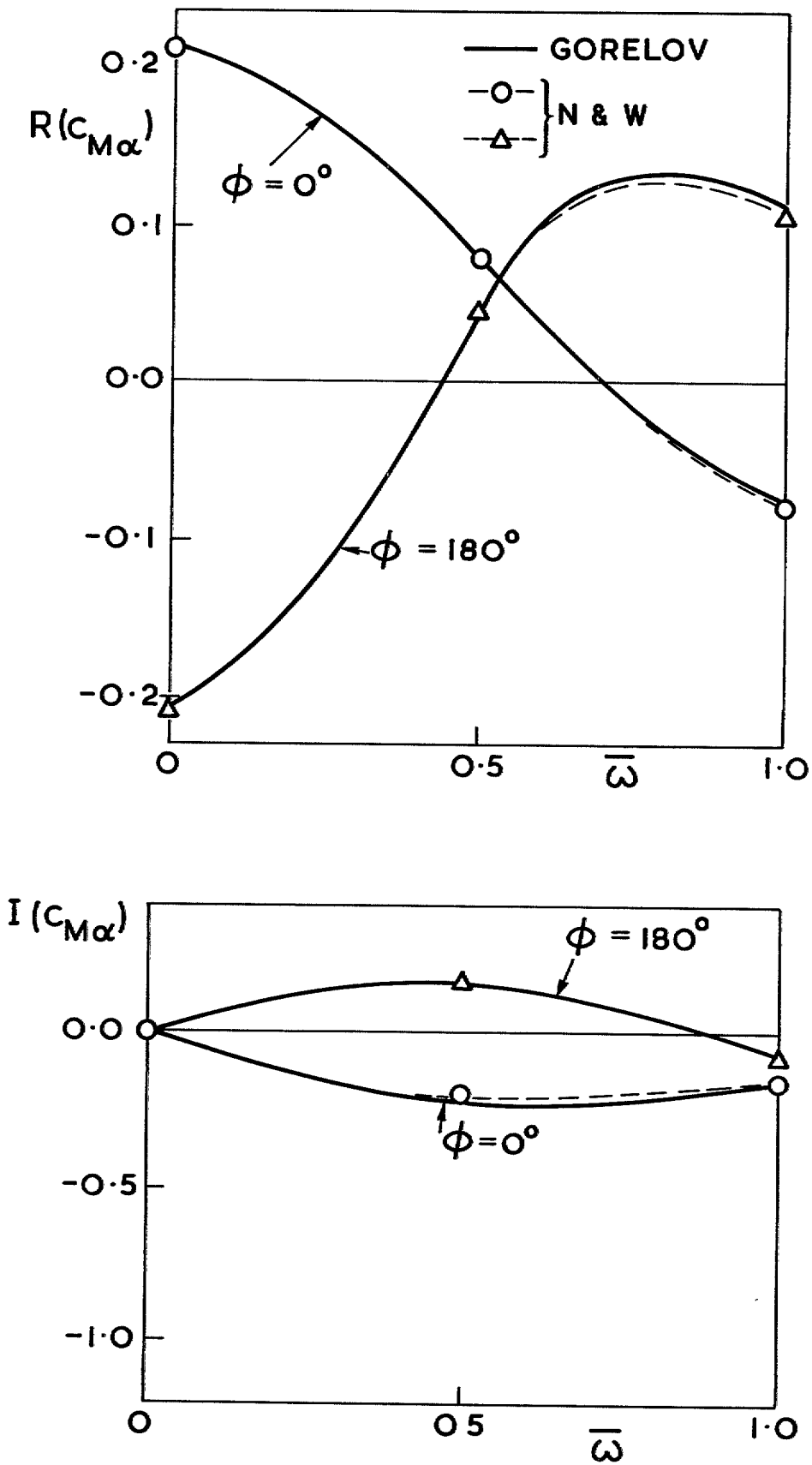


FIG. 6. Comparison with Gorelov; moment coefficient due to torsion. $M = 1.2$, $s/c = 1.0$, $\theta = 0^\circ$, $x_n = 0.0$, $N = 21$.

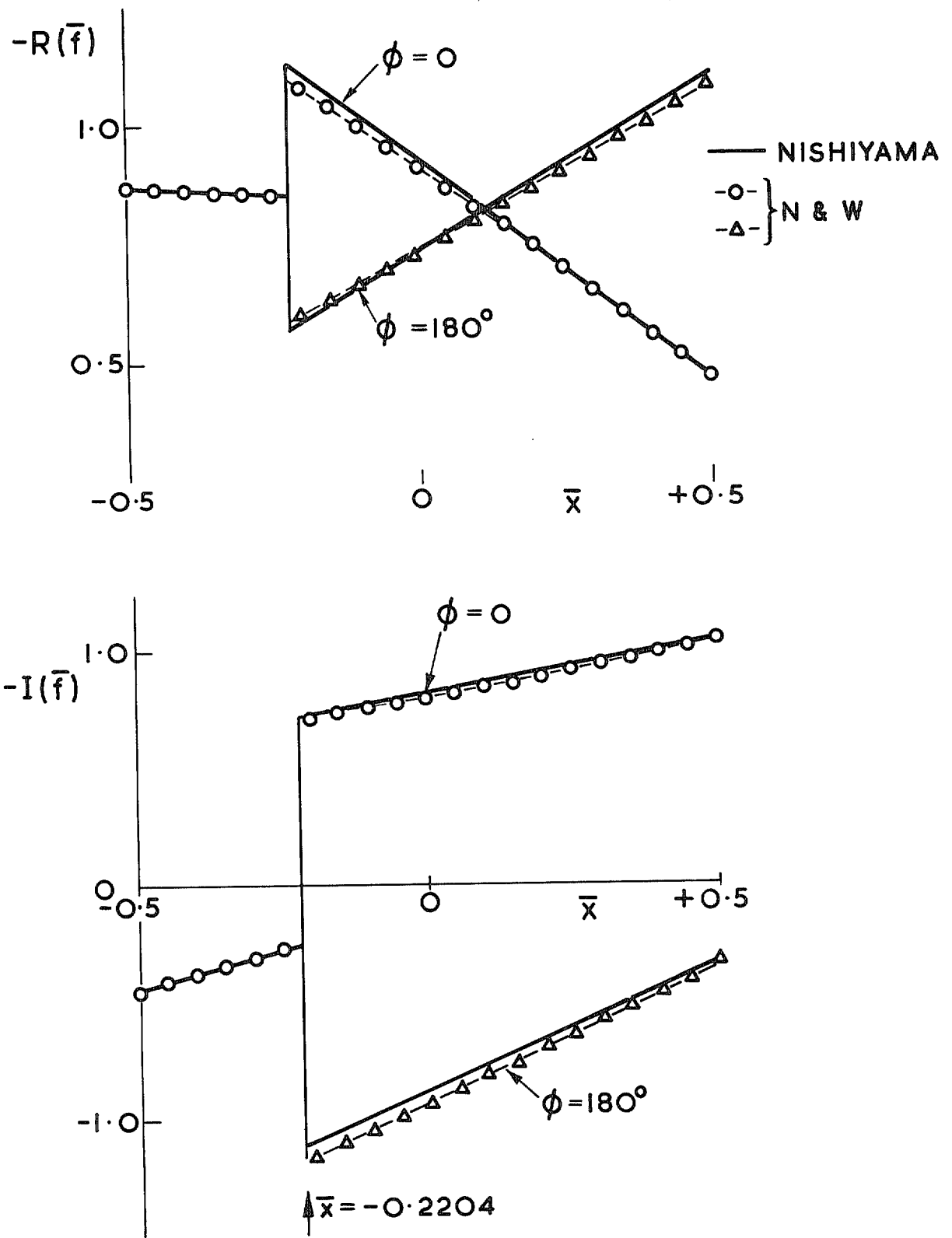


FIG. 7. Comparison with Nishiyama and Kikuchi; pressure difference for torsion. $M = 2.5$, $s/c = 1.0$, $\theta = 60^\circ$, $\bar{\omega} = 1.0$, $x_n = 0.0$, $N = 21$.

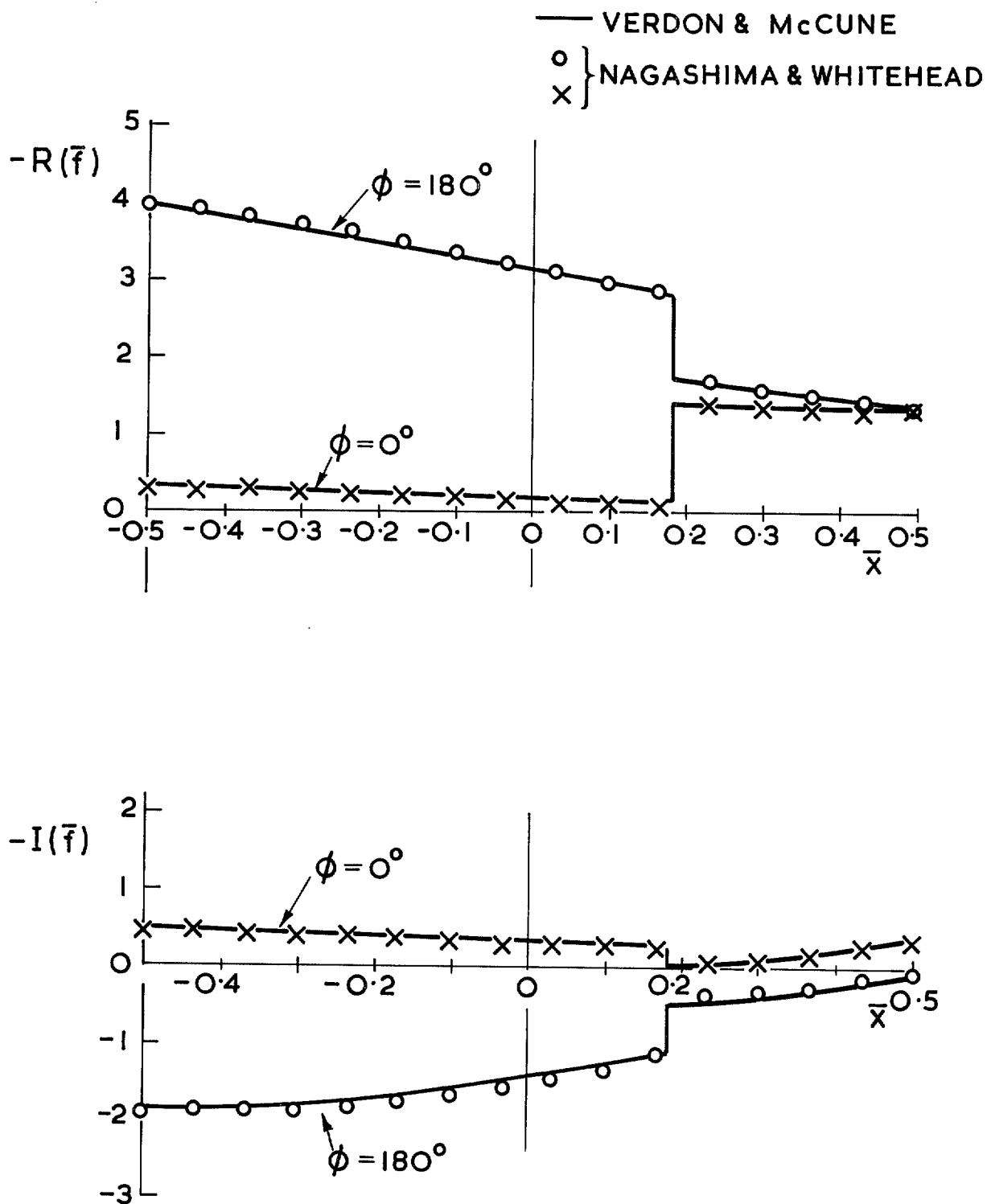


FIG. 8. Pressure distribution for torsional vibration; comparison with Verdon and McCune. Cascade A.
 $M = 1.3454$, $s/c = 0.7889$, $\theta = 59.53^\circ$, $\bar{\omega} = 0.6021$, $x_n = 0.0$, $N = 16$.

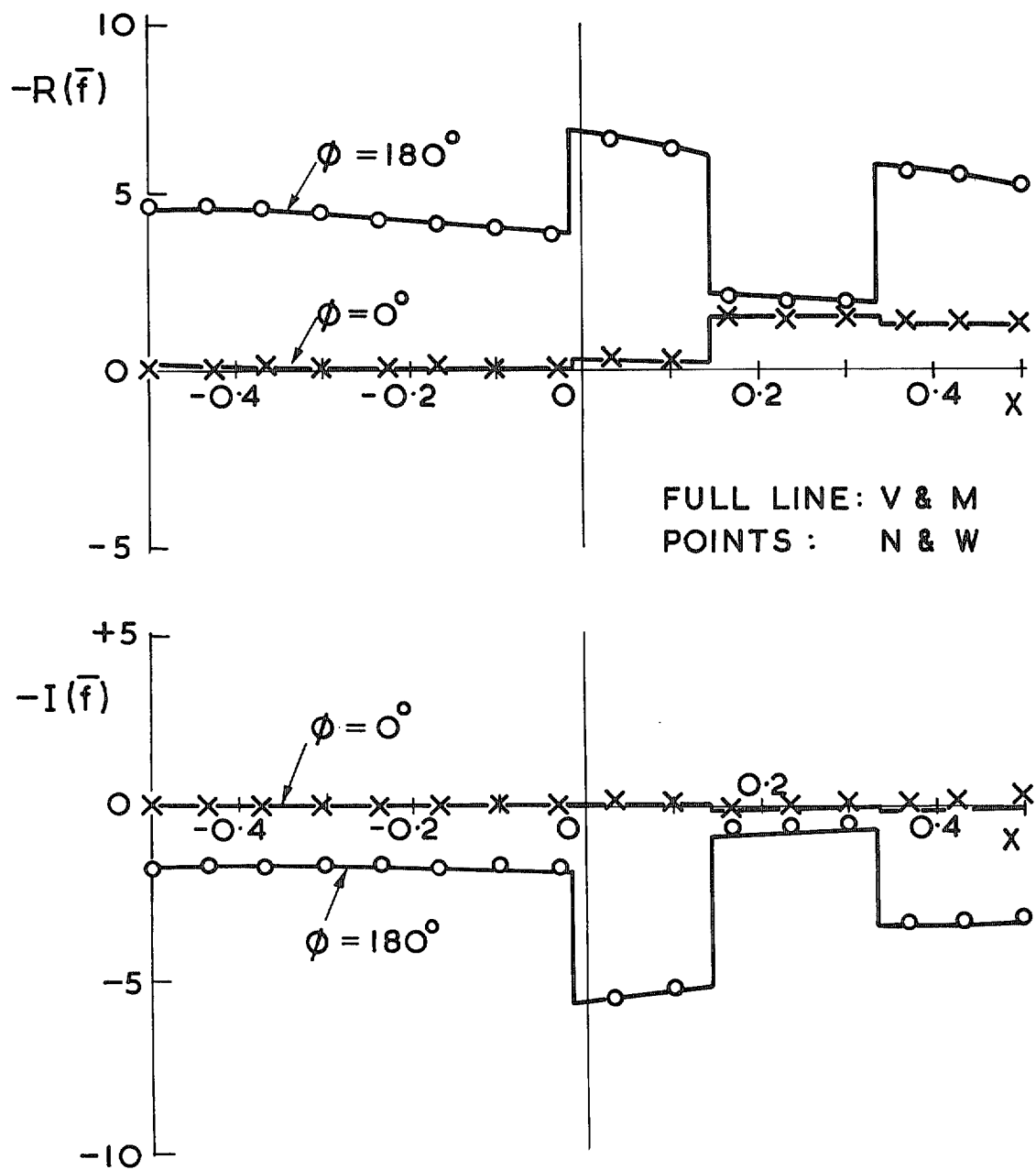


FIG. 9. Pressure distribution for torsional vibration; comparison with Verdon and McCune. Cascade B.
 $M = 1.2806$, $s/c = 0.6708$, $\theta = 63.43^\circ$, $\bar{\omega} = 0.50$, $x_\eta = 0.0$, $N = 16$.

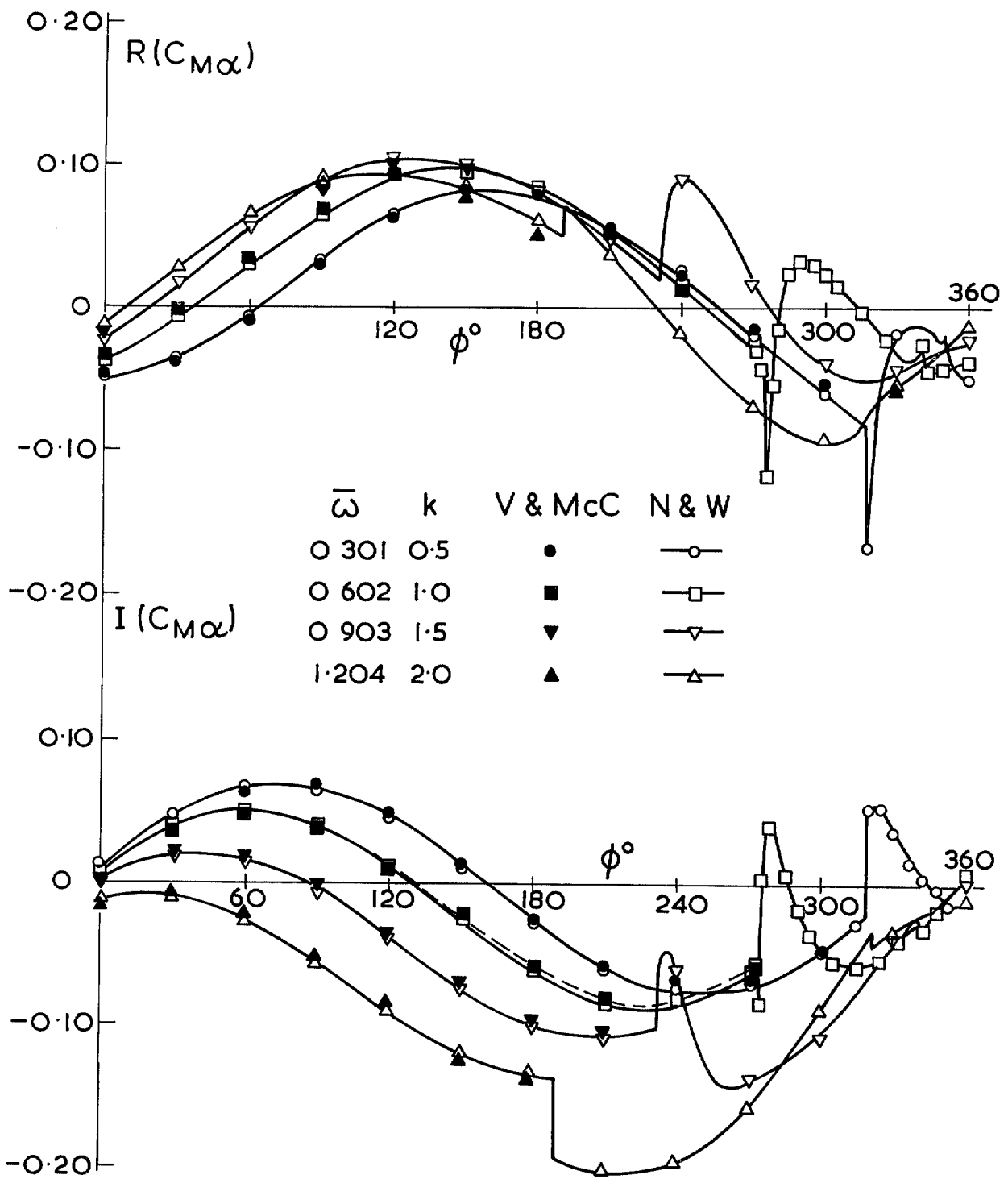


FIG. 10. Comparison with Verdon and McCune. Cascade A. $M = 1.3454$, $s/c = 0.7889$, $\theta = 59.53^\circ$, $x_\eta = 0.0$, $N = 16$.

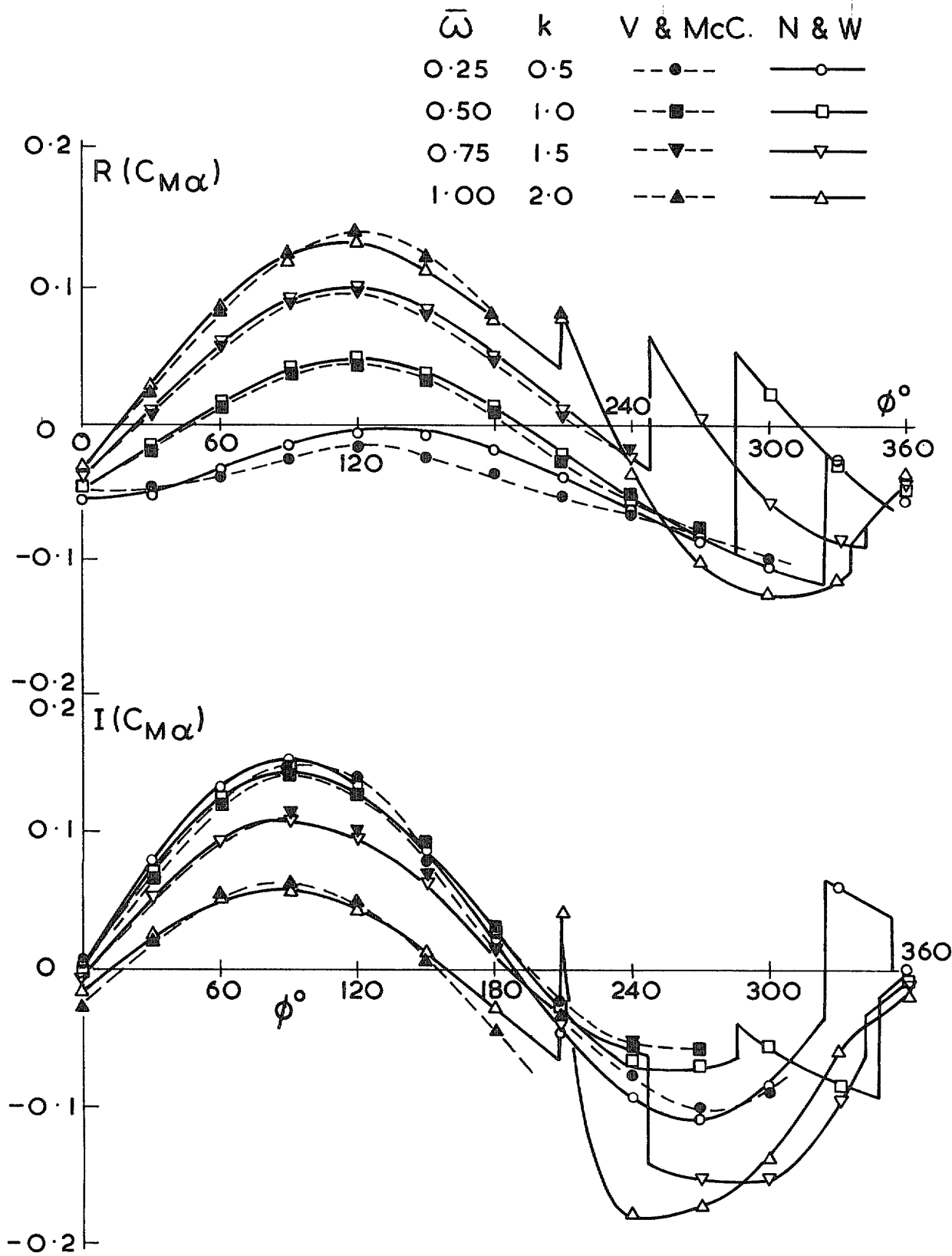


FIG. 11. Comparison with Verdon and McCune. Cascade B. $M = 1.2806$, $s/c = 0.6708$, $\theta = 63.43^\circ$, $x_\eta = 0.0$, $N = 16$.

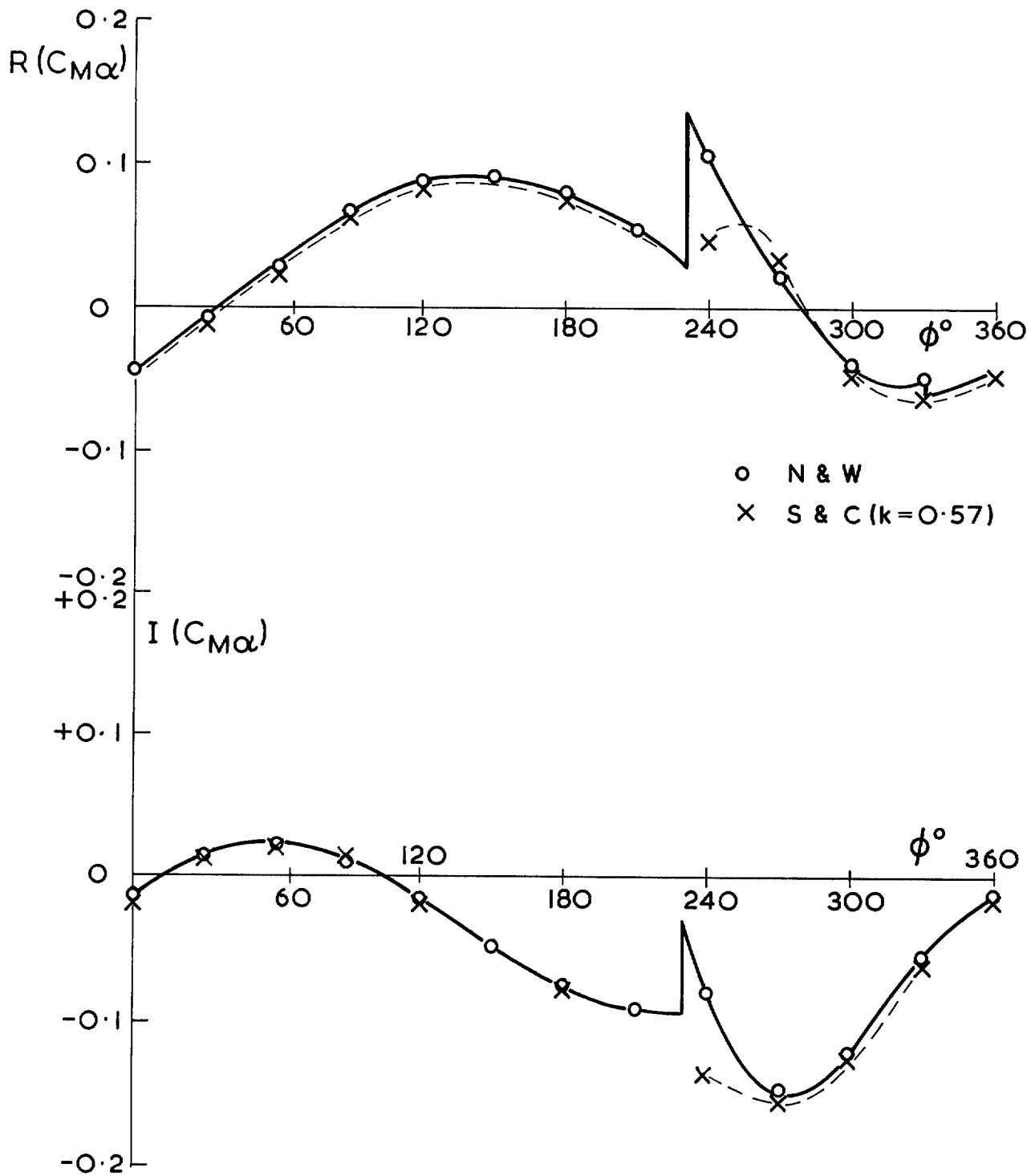


FIG. 12. Comparison with Snyder and Commerford. $M = 1.43$, $s/c = 0.752$, $\theta = 67^\circ$, $x_\eta = 0.0$, $\bar{\omega} = 1.02$, $N = 16$.

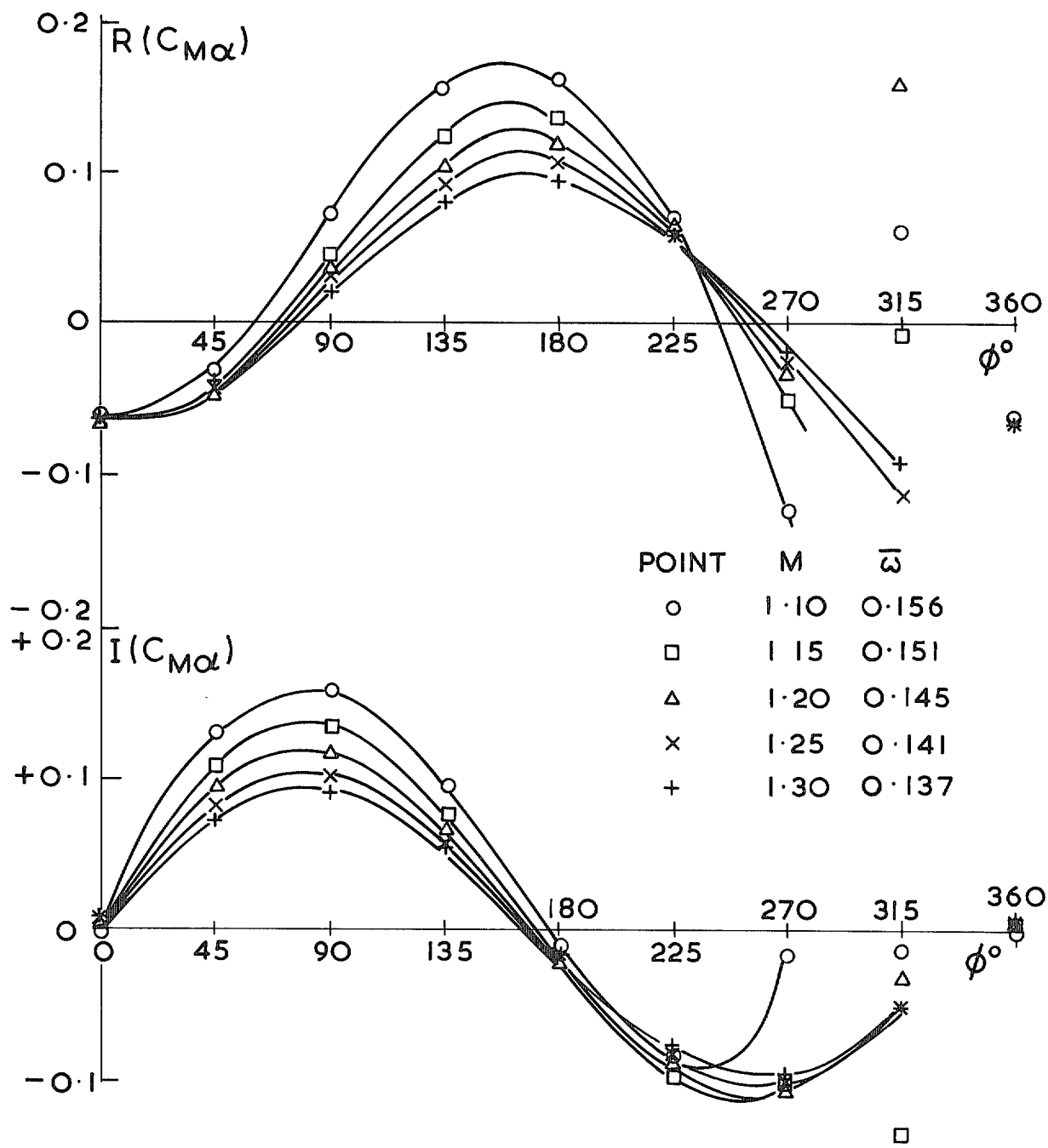


FIG. 13. Results for comparison with experiment. $s/c = 1.005$, $\theta = 60^\circ$, $x_n = 0.0$, $N = 11$.

© Crown copyright 1978

First published 1978

HER MAJESTY'S STATIONERY OFFICE

Government Bookshops

49 High Holborn, London WC1V 6HE
13a Castle Street, Edinburgh EH2 3AR
41 The Hayes, Cardiff CF1 1JW
Brazenose Street, Manchester M60 8AS
Southey House, Wine Street, Bristol BS1 2BQ
258 Broad Street, Birmingham B1 2HE
80 Chichester Street, Belfast BT1 4JY

*Government publications are also available
through booksellers*